

CONTINUOUS-FLOW METHODOLOGIES FOR COPPER-CATALYZED REACTIONS

PhD Thesis

Ádám Georgiádes

Supervisors:

Prof. Dr. Ferenc Fülöp

Dr. Sándor Ötvös



University of Szeged

Institute of Pharmaceutical Chemistry

2019

Table of contents

List of publications and lectures.....	ii
Papers related to the thesis.....	ii
Other papers.....	ii
Scientific lectures related to the thesis	iii
Other scientific lectures	v
Abbreviations	vi
1. INTRODUCTION AND AIMS	1
2. LITERATURE SURVEY	3
2.1 Copper-catalyzed syntheses	3
2.1.1 <i>Synthesis of aniline derivatives and aryl azides from aryl halides</i>	3
2.1.2 <i>Synthetic strategies towards aromatic azo compounds</i>	5
2.1.3 <i>Synthetic strategies towards pyrazoles</i>	8
2.2 Characteristic features of continuous-flow reaction technology	10
2.2.1 <i>Precise parameter control</i>	10
2.2.2 <i>New chemical parameter spaces</i>	12
2.2.3 <i>Continuous-flow multi-step transformations</i>	14
3. EXPERIMENTAL SECTION	16
3.1 General Information	16
3.2 General Procedure for the Flow Reactions	16
3.2.1 <i>Reactions with copper powder as catalytic source</i>	16
3.2.2 <i>Reactions with copper salts as catalytic source</i>	16
3.3 Determination of residence times	17
4. RESULTS AND DISCUSSION	18
4.1 Controlled transformations of aryl halides	18
4.1.1 <i>Optimization</i>	18
4.1.2 <i>Synthesis of aryl amines and aryl azides</i>	23
4.2 New parameter spaces for the oxidative homocoupling of aniline derivatives	26
4.2.1 <i>Reactions mediated by copper powder</i>	26
4.2.2 <i>Cu(II)Fe(II)-layered double hydroxide, as solid base catalyst</i>	31
4.3 Multi-step synthesis of 3,5-disubstituted pyrazoles	35
4.3.1 <i>Step-by-step optimization</i>	35
4.3.2 <i>Telescoped pyrazole synthesis</i>	38
5. SUMMARY	42
Acknowledgements	44
References.....	45
Appendix.....	49

List of publications and lectures

Papers related to the thesis

- I. Ádám Georgiádes, Sándor B. Ötvös, Ferenc Fülöp:
Exploring new parameter spaces for the oxidative homocoupling of aniline derivatives: sustainable synthesis of azobenzenes in a flow system
ACS Sustainable Chem. Eng. **2015**, *3*, 3388-3397. IF.: 5.267
- II. Sándor B. Ötvös, Ádám Georgiádes, Rebeka Mészáros, Koppány Kis, István Pálinkó, Ferenc Fülöp:
Continuous-flow oxidative homocouplings without auxiliary substances: Exploiting a solid base catalyst
J. Catal. **2017**, *348*, 90-99. IF.: 6.759
- III. Ádám Georgiádes, Sándor B. Ötvös, Ferenc Fülöp:
Controlled transformations of aryl halides in a flow system: selective synthesis of aryl azides and aniline derivatives
Adv. Synth. Catal. **2018**, *360*, 1841-1849. IF.: 5.451 (2018)
- IV. Sándor B. Ötvös, Ádám Georgiádes, Dániel Ozsvár, Ferenc Fülöp:
Continuous-flow synthesis of 3,5-disubstituted pyrazoles via sequential alkyne homocoupling and Cope-type hydroamination
RSC Advances, **2019**, *9*, 8197-8203. IF.: 3.049 (2018)

Other papers

- V. Sándor B. Ötvös, Ádám Georgiádes, István M. Mándity, Loránd Kiss, Ferenc Fülöp:
Efficient continuous-flow synthesis of novel 1,2,3-triazole-substituted β -aminocyclohexanecarboxylic acid derivatives with gram-scale production
Beilstein J. Org. Chem. **2013**, *9*, 1508-1516. IF.: 2.801
- VI. Sándor B. Ötvös, Gábor Hatoss, Ádám Georgiádes, Szabolcs Kovács, István M. Mándity, Zoltán Novák, Ferenc Fülöp:
Continuous-flow azide–alkyne cycloadditions with an effective bimetallic catalyst and a simple scavenger system
RSC Advances **2014**, *4*, 46666-46674. IF: 3.840
- VII. Sándor B. Ötvös, Ádám Georgiádes, Mónika Ádok-Sipiczki, Rebeka Mészáros, István Pálinkó, Pál Sipos, Ferenc Fülöp:
A layered double hydroxide, a synthetically useful heterogeneous catalyst for azide–alkyne cycloadditions in a continuous-flow reactor
Applied Catalysis A **2015**, *501*, 63-73. IF: 4.012

Cumulative impact factor: 31.179

Scientific lectures related to the thesis

1. Georgiádes Ádám, Ötvös Sándor, Fülöp Ferenc:
Aromás azovegyületek szelektív szintézise folyamatos áramú technikával
MTA Heterociklusos Kémiai Munkabizottság Ülése, Balatonszemes, Hungary, 27-29 May 2015.
2. Georgiádes Ádám, Ötvös Sándor, Fülöp Ferenc:
Gyógyszerkémiai paraméterter-bővítés áramlásos technikával – aromás azovegyületek szelektív szintézise
Gyógyszerkémiai és Gyógyszertechnológiai Szimpózium, Herceghalom, Hungary, 17-18 September 2015.
3. Ádám Georgiádes, Sándor B. Ötvös, Rebeka Mészáros, Mónika Ádok-Sipiczki, István Pálinkó, Pál Sipos, Ferenc Fülöp
A layered double hydroxide, an efficient heterogeneous catalyst for continuous-flow cycloadditions and oxidative homocouplings
5th Conference on Frontiers in Organic Synthesis Technology, Budapest, Hungary, 21-23 October 2015.
4. Georgiádes Ádám, Ötvös Sándor, Mészáros Rebeka, Kis Koppány, Pálinkó István, Fülöp Ferenc:
Környezettudatos oxidatív homokapcsolási reakciók áramlásos reaktorban hozzáadott bázis nélkül
MTA Heterociklusos Kémiai Munkabizottság Ülése, Balatonszemes, Hungary, 18-20 May 2016.
5. Ádám Georgiádes, Sándor B. Ötvös, Rebeka Mészáros, Ferenc Fülöp
In search of the right path – diversity-oriented aryl azide and arylamine synthesis in continuous-flow
9th Asian-European Symposium on Metal-Mediated Efficient Organic Synthesis, Stockholm, Sweden, 4-7 September 2016.
6. Georgiádes Ádám, Ötvös Sándor, Fülöp Ferenc:
Környezettudatos szintézismódszerek megvalósítása folyamatos áramú technikával
A Tudomány Ünnepe (Szegedi Akadémiai Bizottság Gyógyszerészeti és Kémiai Szakbizottságának közös előadóülése), Szeged, Hungary, 8 November 2016.
7. Georgiádes Ádám
Arilhalogenidek és acetilének réz-katalizált többlépéses in continuo átalakításai
Patonay Tamás-Díj pályázat, Budapest, Hungary, 18 November 2016.
8. Georgiádes Ádám, Ötvös Sándor, Fülöp Ferenc:
Arilazidok és anilinszármazékok diverzitásorientált áramlásos szintézise

MTA Heterociklusos Kémiai Munkabizottság Ülése, Balatonszemes, Hungary, 15-17 May 2017.

9. Ádám Georgiádes, Sándor B. Ötvös, Ferenc Fülöp
Multi-step in continuo synthesis of 3,5-disubstituted pyrazoles
XVII International Conference on Heterocycles in Bioorganic Chemistry, Galway, Ireland, 28-31 May 2017.
10. Ádám Georgiádes, Sándor B. Ötvös, Ferenc Fülöp
Diversity-oriented synthesis of aryl azides and arylamines in a strictly controlled continuous-flow system
18th Tetrahedron Symposium – New Developments in Organic Chemistry, Budapest, Hungary, 27-30 June 2017.
11. Sándor B. Ötvös, Ádám Georgiádes, Rebeka Mészáros, Koppány Kis, István Pálinkó, Ferenc Fülöp
Continuous-flow oxidative homocouplings without auxiliary substances: exploiting a solid base catalyst
18th Tetrahedron Symposium – New Developments in Organic Chemistry, Budapest, Hungary, 27-30. June 2017.
12. Georgiádes Ádám:
Aromás azovegyületek környezettudatos előállítása áramlásos reaktorban
A Tudomány Ünnepe (Szegedi Akadémiai Bizottság Gyógyszerészeti és Kémiai Szakbizottságának közös előadóülése), Szeged, Hungary, 9 November 2017.
13. Georgiádes Ádám:
Alkinek értékes heterociklusokká történő többlépéses átalakítása áramlásos rendszerben
ÚNKP Előadónap, Szeged, Hungary, 17 May 2018.
14. Georgiádes Ádám, Ozsvár Dániel, Ötvös Sándor, Fülöp Ferenc:
3,5-Diszubsztituált pirazolok in continuo előállítása 1,3-diin intermediereken keresztül
MTA Heterociklusos Kémiai Munkabizottság Ülése, Balatonszemes, Hungary, 6-8 June 2018.

Other scientific lectures

15. Sándor B. Ötvös, István M. Mándity, Ádám Georgiádes, Lóránd Kiss, Ferenc Fülöp:
Safe, efficient and scaleable synthesis of novel potentially bioactive 1,2,3-triazoles in flow
4th Conference on Frontiers in Organic Synthesis Technology, Budapest, Hungary, 16-18 October 2013. Abstr.: p. 26-27.
16. Georgiádes Ádám:
1,2,3-Triazolok, mint potenciálisan bioaktív vegyületek szintézise folyamatos áramú technikával
1st Innovation in Science 2014 – Doctoral Student Conference, Szeged, Hungary, 2-3 May 2014.
17. Sándor B. Ötvös, Ádám Georgiádes, István M. Mándity, Lóránd Kiss, Ferenc Fülöp
Efficient continuous-flow synthesis of 1,2,3-triazole-substituted β -amino acid derivatives as novel potentially bioactive compounds
50th International Conference on Medicinal Chemistry, Rouen, France, 2-4 July 2014.

Abbreviations

API	active pharmaceutical ingredient
CF	continuous-flow
cGMP	current good manufacturing practices
conv.	conversion
DFT	density functional theory
DIEA	<i>N,N</i> -diisopropylethylamine
DMEDA	<i>N,N'</i> -dimethylethylenediamine
DMSO	dimethyl sulfoxide
equiv.	equivalent
HPLC	high-performance liquid chromatography
LDH	layered double hydroxide
MeCN	acetonitrile
MS	mass spectrometry
NMR	nuclear magnetic resonance
<i>p</i>	pressure
PIDA	phenyliodine(III) diacetate
select.	selectivity
<i>t</i> BuOI	<i>tert</i> -butyl hypoiodite
TEA	triethylamine
TMEDA	<i>N,N,N',N'</i> -tetramethylethylenediamine

1. INTRODUCTION AND AIMS

Despite the exponential development of science and technology, synthetic chemistry laboratories are still using more than 100-year-old glassware, work-up, and purifying techniques. This synthetic routine restricts the extensive investigation of the chemical parameter space and the possibility for technological improvements. At the end of the previous century, the harmful economic and environmental effects of the product-centered industrial manufacture had been recognized and led to a paradigm shift.^[1, 2] A new chemical philosophy has emerged, patronizing highly selective and economical syntheses, reducing by-products, minimizing waste, and improving plant safety. However, the principles of green and sustainable chemical synthesis and the laboratory practice did not evolve together.

Continuous production is a long-established strategy in the industry: oil refining, synthetic fiber manufacturing, and papermaking have been applying uninterrupted methods for centuries. The application of continuous-flow (CF) processes in the synthetic chemistry appeared only two decades ago, offering significant advantages over the conventional segmented techniques.^[3] Owing to their technological possibilities, they allow simple, safe, and precise fine-tuning of the reaction conditions. Moreover, the enhanced heat and mass transfer provides an impaired level of reaction control.^[4-6] Flow chemistry also offers in-line analysis, purification, and even formulation.^[7, 8] Thus, CF technology may serve as an avenue towards the technological revolution of chemical synthesis.

Since the first examples, CF synthesis methods have gone through an extraordinary progression. Due to their advantages over conventional techniques and applicability in difficult and sensitive reactions, CF methods became an impressive tool for synthetic chemistry and proved not to be only a transient vogue.^[9] The borderline between segmented and flow processes has become more apparent, making it straightforward to decide whether the application of a CF process is beneficial or unnecessary. Nowadays, performing the entire synthesis of complex compounds (such as APIs) as uninterrupted continuous-flow processes is an actual endeavor.^[10, 11]

Our aim was to apply continuous-flow technology, focusing attention on copper-catalyzed reactions to explore otherwise hidden parameter spaces from classical batch syntheses and to develop efficient, selective, safe, and sustainable synthesis methods. Highlighting its applicability in organic chemistry, we investigated the CF technology in three reaction systems: *(i)* highly controlled synthesis of aryl azides and aniline derivatives from haloarenes; *(ii)* extension of the chemical parameter spaces for the oxidative homocoupling

of aniline derivatives; (iii) two-step *in continuo* synthesis of 3,5-disubstituted pyrazoles. Each work represents a case study how CF processes can improve synthetic reaction technology.

Copper-mediated nitrogenation of aryl halides with sodium azide can result in either aryl azides or aniline derivatives, which are valuable compounds in both synthetic and pharmaceutical chemistry.^[12, 13] The selectivity of these transformations strongly depends not only on the materials (i.e., catalyst, solvent, different auxiliaries), but also on the reaction time and temperature applied, leading to contradictory literature results and ambiguity of the exact effects of the reaction conditions. Therefore, we planned to exploit the advantages of a strictly controlled flow reactor and develop a practical method for the selective synthesis of both aryl azides and aniline derivatives starting from the same haloarenes. We aimed to adjust the selectivity by means of fine-tuning the reaction conditions.

Azobenzenes are not only valuable compounds in the chemical industry, but also in medicinal chemistry and biotechnology.^[14, 15] Due to reactivity issues and the facile formation of side-products, the batch synthesis of these compounds deals with non-optimal selectivity and often requires long reaction times and special reaction conditions.^[16] We proposed to explore novel parameter spaces for the chemical intensification of the copper-catalyzed oxidative homocoupling of arylamines, and to develop a simple, efficient, and selective CF method. As a further step towards sustainability, we envisioned to apply a solid base catalyst to avoid the need for any auxiliary substances. We aimed to explore the role of Cu(II)Fe(III)-LDH, a hydrotalcite-like material as a solid bifunctional catalyst in the oxidative homocoupling reactions of aniline derivatives.

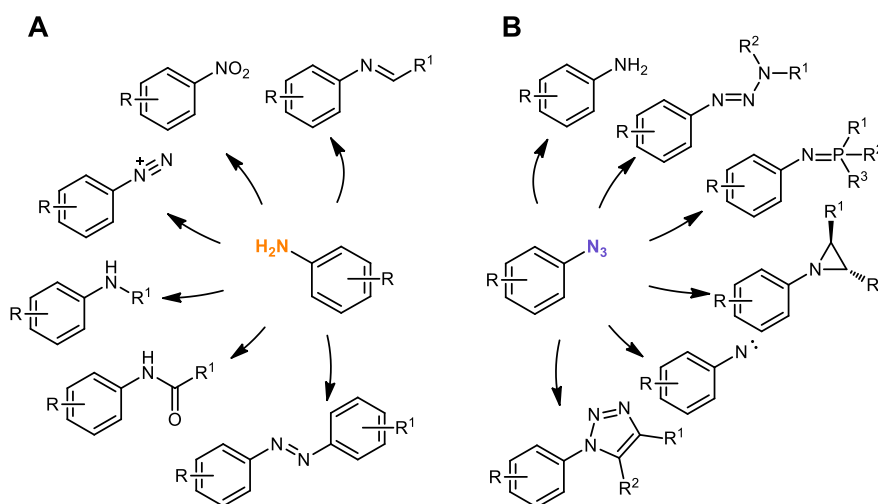
The pyrazole motif can be found in several pharmaceutically active compounds with a wide range of therapeutic effects.^[17] In addition, pyrazole derivatives have important applications as chelating agents, fluorophores, and agrochemicals. The classical methods for the synthesis of pyrazoles typically apply harsh reaction conditions and necessitate environmentally unfriendly reactants and/or special starting materials.^[18] Recently, the intermolecular Cope-type hydroamination of 1,3-dialkynes with hydrazine was described, affording 3,5-disubstituted pyrazoles.^[19] The reaction occurs under mild conditions and does not require catalyst or any additives. Flow chemistry is a valuable toolbox to perform multistep synthesis. Therefore, we intended to design a multistep flow synthesis for the transformation of terminal alkynes into 3,5-disubstituted pyrazoles without the isolation of the corresponding diyne intermediate.

2. LITERATURE SURVEY

2.1 Copper-catalyzed syntheses

2.1.1 Synthesis of aniline derivatives and aryl azides from aryl halides

Aryl amines and aryl azides have indisputable value with wide-ranging applications in diverse areas of chemistry. Both can be transformed into numerous chemical structures (Scheme 1), and they are fundamental in the construction of various *N*-heterocycles.^[12, 13] Traditionally, aniline derivatives are starting materials for the synthesis of dyes, pigments, agricultural materials, rubber products, and other polymers.^[20] Many pharmaceutically active compounds contain amino-substituted aromatic moiety, and a large number of drugs can be synthesized from anilines presenting a broad spectrum of therapy. Since the recognition of their importance in click chemistry, the azide function is an attractive moiety in biomedical chemistry, material science, radiochemistry, and drug discovery.^[21, 22]



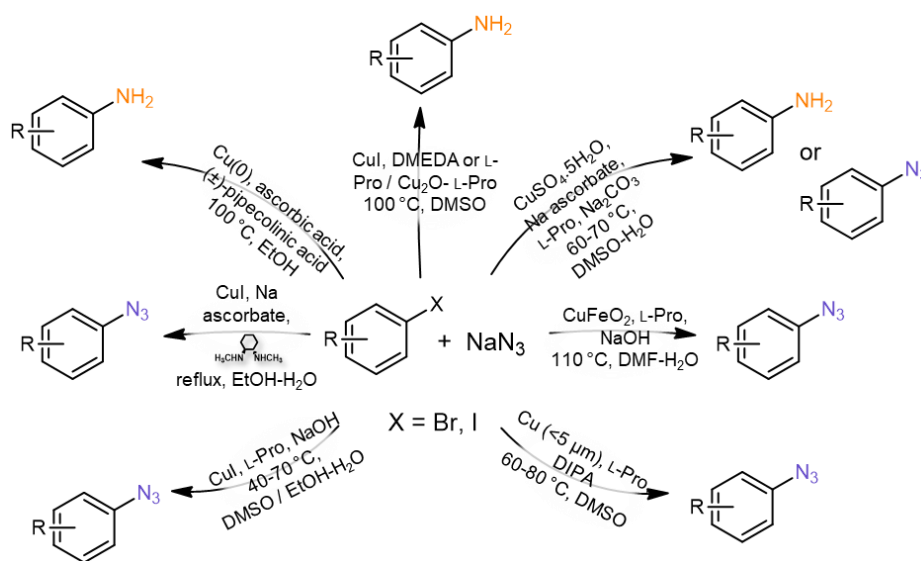
Scheme 1. Examples for the transformations of aryl amines (A) and aryl azides (B)^[12, 13]

As the most popular and recent methods towards aryl amines, the reduction of nitro compounds,^[23-26] the transformation of aromatic boronic acids,^[27-32] and the direct amination of aryl halides^[33-39] can be highlighted. In recent years, sophisticated methods were developed. However, these reactions require expensive starting materials and/or ligands, harsh reaction conditions, and result in inorganic by-products in several cases.

Aryl azides can be prepared through many synthetic strategies, such as transformation of aryl diazonium compounds, nucleophilic substitution of halogens by azide anion, reaction with organometallic compounds (Grignard or lithium reagents), diazo transfer reaction, diazotization of hydrazines, reaction of nitrosoarenes with hydrogen azide, and rearrangement of triazenes.^[13] Most of the methods were developed in the previous century and they

generally deal with a number of disadvantages, such as unstable, toxic and/or explosive reagents and reactants, and harsh conditions.

Aryl halides are valuable starting compounds for the synthesis of both aniline derivatives and aryl amines. Recently, copper-catalyzed reactions of aryl halides with sodium azide came into the focus of interest, due to the price, easy availability, and low toxicity of common copper salts and haloarenes.^[40-46] However, these reactions can result in either aryl azides or anilines, and related literature data are confusing with respect to product selectivity and the conditions applied (Scheme 2).



Scheme 2. Copper-mediated reactions between aryl halides and sodium azide^[40-46]

In 2004, Ma and Zhu found that CuI/L-proline can catalyze the reaction of aryl halides with sodium azide, affording the efficient synthesis of aryl azides.^[40] The reaction occurred at relatively mild conditions of 40–70 °C and 5–24 h reaction time. The research group also noticed significant correlation in the reactivity between the quality of the solvent and the type of the halogen. Later, the catalytic activity of heterogeneous porous Cu(0)/L-proline system was also investigated, achieving similar results^[45] under comparable reaction conditions (60–80 °C, 13–24 h reaction time). Interestingly, in the case of 1-bromo- and 1-chloro-4-iodobenzene, the corresponding aniline derivatives were detected in small amounts. Additionally, CuFeO₂ was also applied as catalyst in an L-proline/NaOH system at slightly higher temperatures (95–115 °C).^[46] In a different study, the haloarene transformation was performed applying CuI as catalytic source and *trans*-*N,N'*-dimethylcyclohexane-1,2-diamine as ligand.^[41] It was found that the addition of sodium ascorbate is essential for full conversion with the concomitant significantly reduced reaction time. A remarkable

solvent dependence was also reported; however, the selectivity was independent from the quality of the halogen substituent.

The first observations for the copper-mediated direct amination of haloarenes with sodium azide were accidental, found in the unsuccessful reproduction of the azidation described above.^[47] Interestingly, in a comprehensive study, Helquist and co-workers investigated the effect of several reaction parameters, and explored the scope of the reaction applying CuI or Cu₂O as the copper source and L-proline or *N,N'*-dimethylethylenediamine (DMEDA) as ligand at 100 °C.^[43] The research group demonstrated that aryl azides can be transformed into the corresponding amines, where the joint presence of CuI and NaN₃ is essential. However, stoichiometric amounts of the copper species were used in their experiments.

The Cu(0)-catalyzed amination of aryl halides in the presence of ascorbic acid and (±)-pipercolinic acid was demonstrated by Alami et al.^[44] According to their suggested mechanism, the corresponding azide is formed as an intermediate in the reaction, then suffers a thermo-initiated N₂ liberation resulting in a nitrene species, which converts to the corresponding amine product. An additional study reported the successful utilization of CuSO₄·5H₂O in combination with ascorbic acid (or Na ascorbate) and various ligands for the synthesis of substituted anilines at temperatures of 60–100 °C, where the catalyst and both additives were essential for the reaction.^[42]

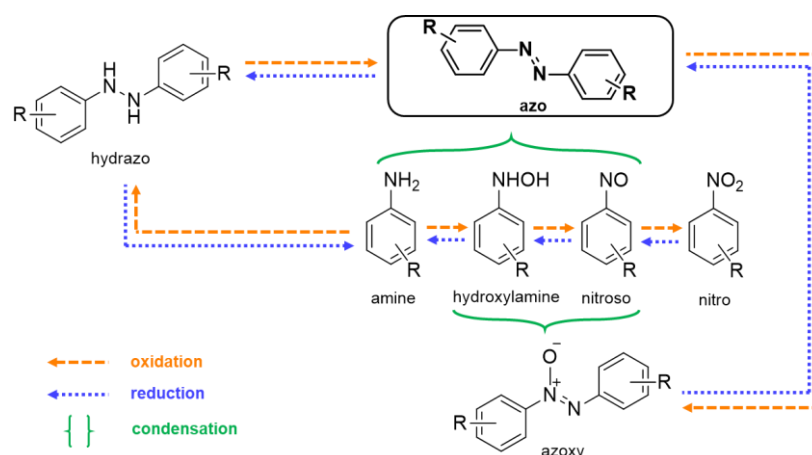
It is evident that the selectivity of the copper-mediated reaction between aryl halides and sodium azide is powerfully influenced by all reaction parameters, such as the solvent, catalytic source, temperature, and reaction time, as well as the type of the halogen and the substitution patterns of the starting materials. The ambiguous results may be explained by facile azide reduction/decomposition;^[42-44] however, the exact effects of the reaction conditions are still unclear. The clarification of the contradictions described above may lie in the strict control over the reaction conditions.

2.1.2 Synthetic strategies towards aromatic azo compounds

Besides their well-known relevance as dyes and indicators,^[48, 49] azobenzenes are valuable compounds in medicinal chemistry. Due to the fact, that the N–N double bond can only be cleaved by the bacteria in the colon, aromatic azo compounds can be used as pro-drugs or drug coating materials in the targeted therapy of the bowel.^[50-53] As a result of the reversible photo-initiated or thermally induced *cis*–*trans* isomerization of the azo function, these compounds are valuable elements of photo-responsive materials. Consequently, they

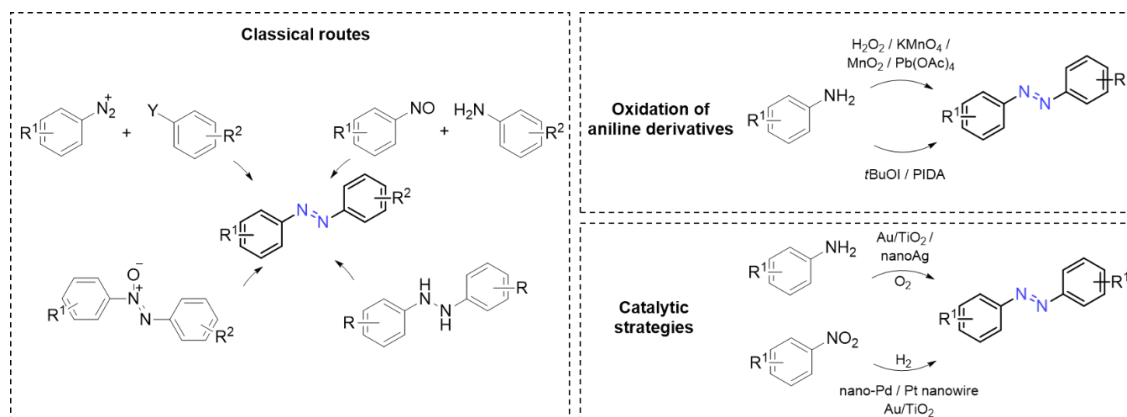
can be utilized for the development of polymers for nonlinear optics,^[54, 55] artificial muscle,^[56] molecular machines,^[14] and solar thermal energy storages.^[57-59]

Aromatic azo compounds are members of a complex redox network (Scheme 3).^[60-62] In this complicated system, several reaction pathways could lead towards azobenzenes, such as the oxidation of hydrazo derivatives, the reduction of azoxy species, or the condensation of hydroxylamine with nitroso compounds or aniline derivatives. Thus, it is beyond doubt that selectivity is an essential parameter in the synthesis of azobenzenes. Depending on the strategy and reagents applied, various side-reactions, for example, inefficient condensations, overreduction or overoxidation of azobenzenes, may easily occur leading to selectivity issues. This sensitive equilibrium makes the practical synthesis of aromatic azo compounds a significant challenge.^[16]



Scheme 3. Reaction network and pathways towards azobenzenes

Scheme 4 summarizes the main synthesis strategies towards azobenzenes. As classical routes, azo coupling (the coupling of diazonium salts with activated aromatics), Mills reaction (coupling of primary arylamines with nitroso compounds), the oxidation of hydrazines, and the reduction of azoxy derivatives can be mentioned.^[16] These techniques typically involve special or harsh reaction conditions, such as the use of strong oxidizing agents and strong inorganic acids or bases, which often lead to remarkable by-product formation and inadequate selectivity and productivity rates. The oxidation of aniline derivatives with conventional oxidizing agents, such as KMnO_4 , MnO_2 , H_2O_2 , $\text{Pb}(\text{OAc})_4$ or HgO , usually provides low selectivity with the formation of inorganic by-products. The application of mild oxidants, for example, *tert*-butyl hypoiodite (*t*BuOI)^[63, 64] and phenyliodine(III) diacetate (PIDA),^[65] improves the selectivity rates. However, these methods often require precise temperature control and longer reaction times, and the remaining reduced reagent by-products still lead to difficulties during the work-up and purification steps.



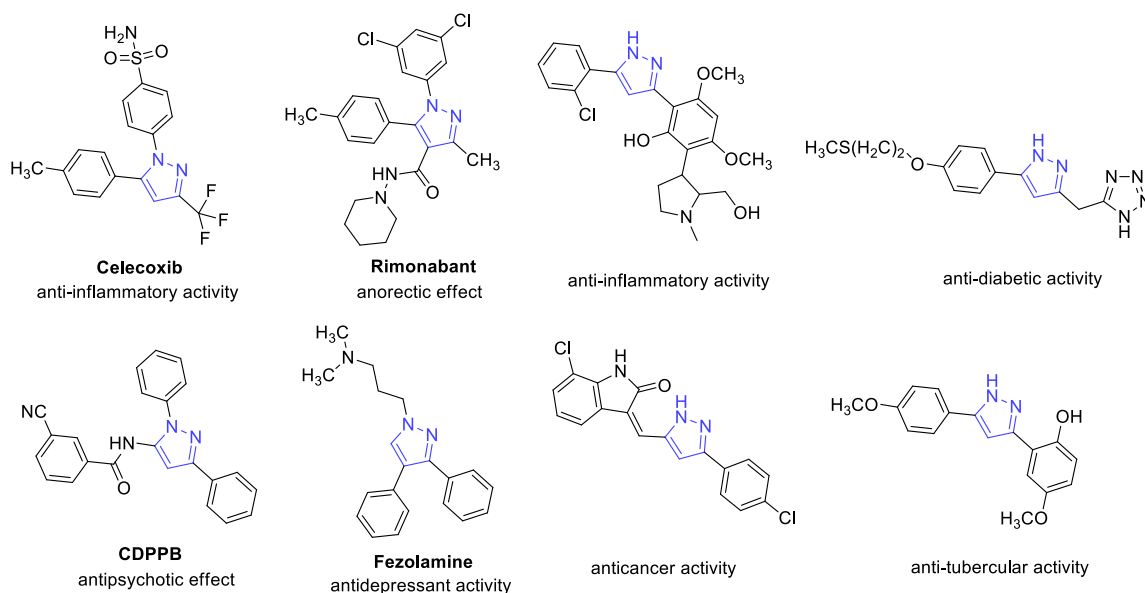
Scheme 4. Synthetic strategies towards azobenzenes

A significant part of the above-mentioned disadvantages can be overcome by utilizing catalytic approaches. Recently, two novel strategies came into the center of interest: the reduction of nitrobenzenes and the oxidation of aniline derivatives. The reductive approach necessitates hydrogen atmosphere and special heterogeneous catalyst systems, such as palladium nanoparticles, platinum nanowire, and Au/MgAl hydrotalcite.^[66-68] The catalytic oxidative pathway was first reported using Au/TiO₂ system and Ag nanoparticles, but the price of the gold and silver catalysts limits the sustainable application of the methods.^[69, 70] Although these catalytic strategies are preferable over conventional methods, the application of H₂ or O₂ gases requires safety precautions and overreductions or overoxidations can still easily occur, leading to non-optimal selectivity and hence, low yields.

In recent years, the copper-catalyzed oxidative dimerization of aniline derivatives brought new opportunities for the synthesis of azobenzenes.^[71-75] Typically, copper(I) halides were used as catalytic copper source in the presence of different bases, ligands, and oxidants. As base, pyridine proved to be the most efficient, and the oxidative conditions were achieved by the application of oxidizing agents, oxygen or air atmosphere. Jiao et al. proposed a mechanism of the CuBr₂/pyridine/O₂ catalyst system, in which a copper–ligand–oxygen complex acts as the active specimen through a hydrazine-derived intermediate.^[72] Such copper-catalyzed synthetic approaches are much cleaner, more efficient, and more economical than the above-described methodologies. They apply a cost-effective catalytic system, do not require harsh reaction conditions, such as high temperature and drastic inorganic reactants, and the only by-product of the reaction is water.

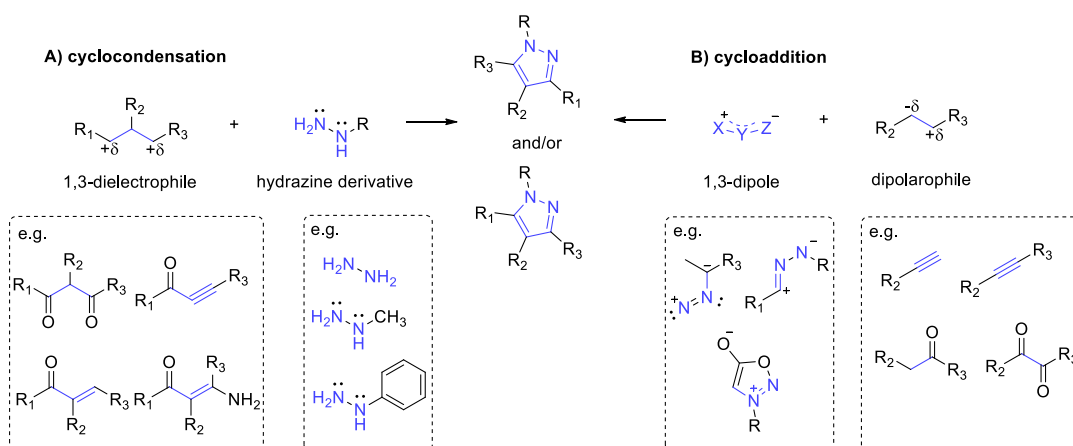
2.1.3 Synthetic strategies towards pyrazoles

Heterocycles, particularly nitrogen-containing rings, have well-known and indisputable importance in synthetic and pharmaceutical chemistry. Pyrazoles, one of the five-membered nitrogen heterocycles, have impressively diverse applications.^[76] As a core structure, pyrazole constitutes a myriad of pharmaceutically active compounds with a wide spectrum of biological activities, such as antihyperglycemic, analgesic, anti-inflammatory, antipyretic, antibacterial, antiviral, antituberculous, and sedative-hypnotic effects (Scheme 5).^[17, 76-82] Besides their relevance as versatile building blocks in organic chemistry and as ligands and chelating agents in coordination chemistry, pyrazoles are valuable as fluorophores and energetic materials.^[83] Furthermore, they can also be used in the agrochemical industry as insecticides, fungicides, and herbicides.^[76]



Scheme 5. A few examples for biologically active pyrazoles

More than a century after the first reported pyrazole synthesis, the classical strategy of the 5-membered ring construction did not change radically.^[84] Two main approaches can be distinguished: the [3+2] cyclocondensation between a hydrazine derivative and a 1,3-dielectrophilic compound (Scheme 6 “A”), and the cycloaddition of 1,3-dipoles and dipolarophiles (Scheme 6 “B”).^[18] 1,3-Dicarbonyl, α,β -unsaturated carbonyl, and related compounds are commonly used 1,3-dielectrophiles. In the more powerful and highly regioselective 1,3-dipolar cycloadditions diazoalkanes, nitrilimines, azomethine imines, and sydnone can be chosen as 1,3-dipoles to react with activated alkenes or alkynes.

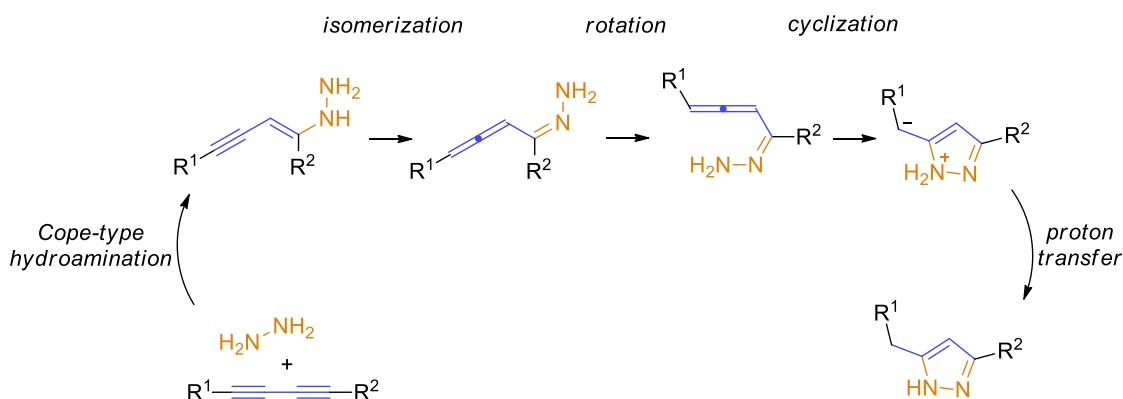


Scheme 6. Main approaches towards pyrazoles

Multicomponent reactions are relevant synthetic strategies towards pyrazoles, where the reactants are formed *in situ*, without isolation or purification of the intermediates. Transition metal catalysts are attractive choices to induce the functionalization of the pyrazole ring through C–C and C–N cross-coupling reactions.

Although both mono- and poly-substituted pyrazoles can be synthesized using these methods, their production typically requires harsh reaction conditions (strong base, high temperature), environmentally unfriendly reactants and/or special starting materials.^[85-90]

Bao and co-workers reported an efficient and mild method for the synthesis of 3,5-disubstituted pyrazoles via a Cope-type hydroamination reaction between 1,3-diynes and hydrazine.^[19] The thermally initiated reaction did not necessitate the presence of an extraneous base or acid. Tang et al. investigated the reaction mechanism and proposed a plausible pathway on the basis of density functional theory (DFT) calculations (Scheme 7).^[91] The reaction starts with the nucleophilic attack of hydrazine onto the diyne core, which results in an allene intermediate. Then this step is followed by electrophilic cyclization yielding a new C–N bond and leading to the pyrazole motif.



Scheme 7. The possible mechanism on the reaction of 1,3-dialkynes and hydrazine^[91]

For CF synthesis of pyrazoles, several examples can be found in the literature including multistep strategies.^[92-95] For instance, Buchwald et al. developed a two-step continuous process, where arylhydrazines were generated *in situ* by a cross-coupling reaction and then immediately transformed into the corresponding *N*-arylpyrazoles through cyclocondensation with 1,3-diketones.^[93] Another example was demonstrated by Ley and co-workers for the synthesis of *N*-arylpyrazoles through a three-step telescoped flow process.^[96] Fully continuous production of pyrazole-containing pharmaceutically active compounds was also demonstrated. For example, the kilogram-scale synthesis of an anticancer drug, prexasertib monolactate, was integrated into a four-step uninterrupted CF process, with a hydrazine condensation reaction as the first step.^[97] As a consequence of the CF technology, this step proceeded with improved safety, affording high yield and purity. Moreover, the method satisfied the criteria of current good manufacturing practices (cGMP), which is a collection of strict regulations for the manufacturing of a drug product.

2.2 Characteristic features of continuous-flow reaction technology

2.2.1 Precise parameter control

In a CF method, chemical transformations take place during the migration of the reagents and reactants through the active reactor zone. Thus, not only temporal, but also spatial changes occur during the progression of the reaction. (Figure 1).^[98]

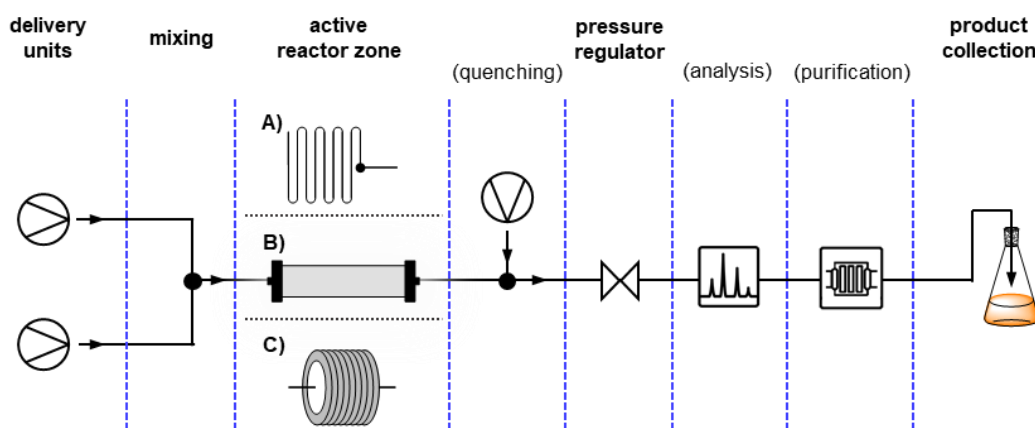


Figure 1. Schematic representation of a CF reactor^[98]

Delivery units allow precise control over the flow rate of the fluids. After the mixing phase, the components enter the active reactor zone, which can be heated and pressurized in an easy and safe manner.^[99] As the compounds leave the active reactor zone, the reaction can be stopped by the addition of a quenching agent.

CF systems enable simple integration of both online and inline analytical tools, for example, infrared spectroscopy, UV/Vis spectroscopy, and mass spectrometry.^[100] Therefore, real-time reaction monitoring can be obtained facilitating the optimization of the reaction parameters and offering a constant quality control. Moreover, the purification and work-up phases can also be implemented into the flow process, such as evaporation, liquid–liquid separation, crystallization, and filtration.^[101] Finally, the pure product will be collected.

Since the classical interpretation of batch production cannot be defined in a CF method, *reaction time* and the *volume of the reaction mixture* terms are not applicable.^[102] For the precise characterization of the reaction conditions, the definition of the residence time was introduced. *Residence time* is the time the reaction mixture spends in the active reactor zone, which is defined by two parameters: it is directly proportional to the *volume of the flow path* in the active reactor zone and inversely proportional to the *flow rate*. Both parameters can easily be modified. Thus, one can precisely regulate the residence time, which can affect not only the conversion but also the chemo- and stereoselectivity of a reaction.^[103]

Reactions involving highly reactive and labile intermediates are problematic to handle in conventional flask-based techniques. They typically require cryogenic conditions to achieve sufficient control over reactivity and selectivity. In contrast, flow chemistry allows precise control over reaction times in the range of milliseconds to seconds, which led to the concept of “flash chemistry”.^[104] For example, Br/Li exchange reactions of bromopyridines and the subsequent transformation of the resulting intermediate require cryogenic conditions to avoid side-reactions. Applying an integrated CF microreactor system, Yoshida and co-workers achieved high selectivity values even at 0 °C. The lithium-substituted intermediate was formed in a highly controlled manner within a very short residence time and was sequentially trapped by introduction of an electrophile. (Figure 2).^[105]

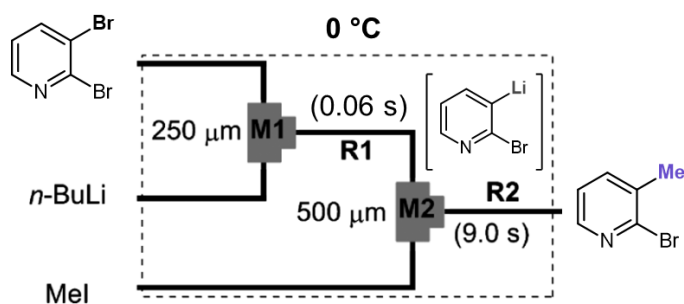


Figure 2. Flow microreactor system for Br/Li exchange reaction^[105]

The small internal dimensions of CF reactors involve high surface to volume ratios, which result in effective heat transfer. This highly controlled thermal energy transfer leads to homogeneous and narrow temperature distribution even in the case of highly exothermic reactions. As Figure 3 shows, the significantly wider thermal profile in batch processes may easily lead to side-reactions providing lower selectivity and yield.^[102, 106] The small internal dimensions also enhance mass transfer. For efficient reaction rates in a flask, a mixing unit should be added, which results turbulence as the main fluid motion pattern. In contrast, CF reactors show improved fluid dynamics.^[107] This generates large interfacial areas between the fluid layers and leads to improved mass transfer by means of diffusion.

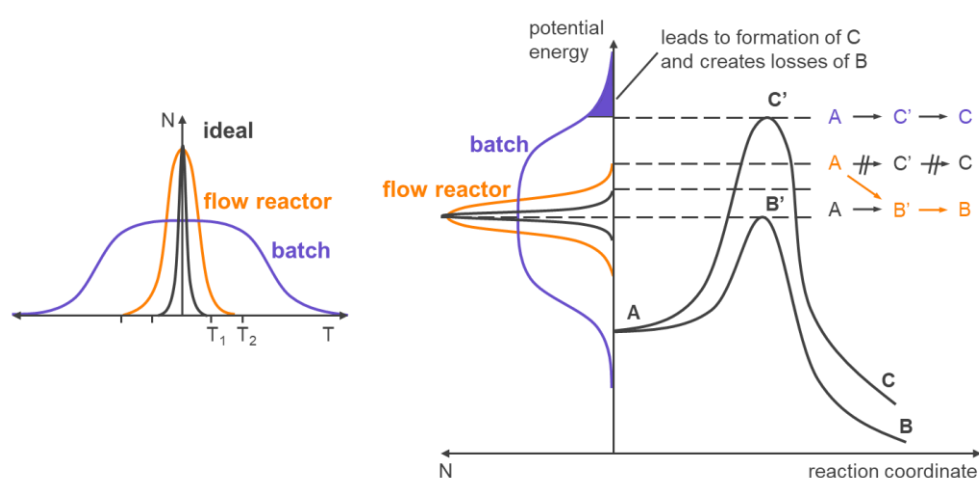


Figure 3. Temperature profiles in batch and CF A: starting material; B: product; C: side-product^[106]

2.2.2 New chemical parameter spaces

As a consequence of the safe and precise parameter control of CF syntheses, so far unknown chemical spaces, so-called novel process windows may reveal, opening up new opportunities in synthetic chemistry.^[4, 108]

Flow chemistry is described as an enabling technology and evolved to serve as a sophisticated toolbox for various synthetic chemical dilemmas. Figure 4 shows the pressure–temperature distribution of current synthetic chemistry techniques.^[99, 109, 110] It is clearly visible that flow chemistry is one of the most promising technologies, since it may cover a wide range of reaction parameters.

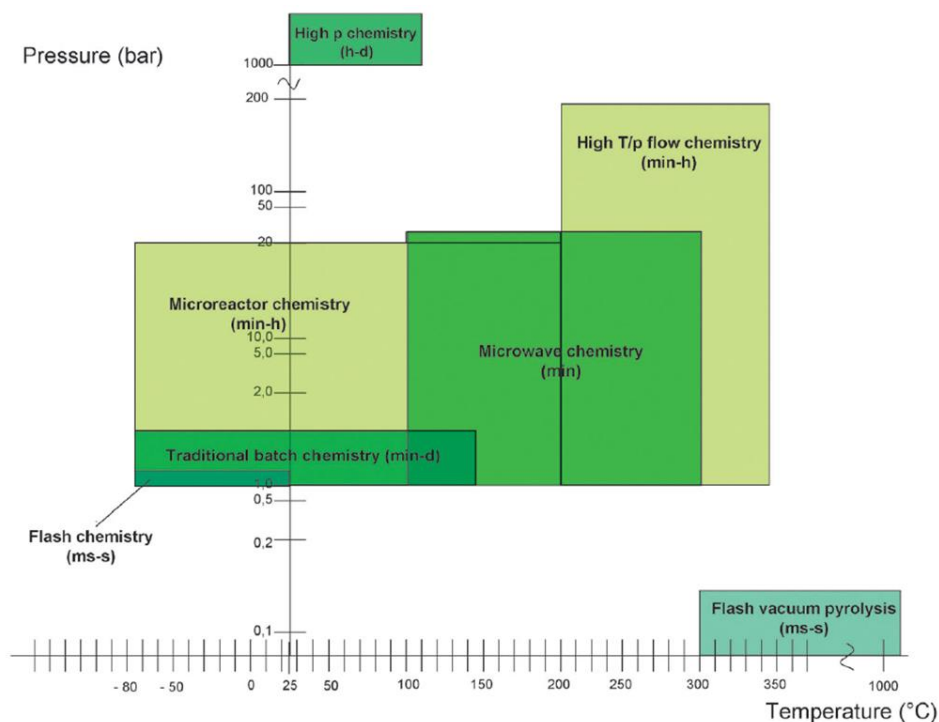


Figure 4. Enabling technologies in synthetic chemistry^[109]

In classical segmented synthetic methods, pressurization is more difficult to implement requiring pressure-resistant autoclaves and involves safety issues. In contrast, lab-scale flow chemistry offers a simple and safe access to high pressures by using commercially available backpressure regulators in the range of 2–200 bar. These accessories allow to reach high pressure and temperature regimes exceeding the critical point of the solvent, leading to supercritical conditions.^[99] Numerous studies demonstrate the applications of high-temperature and high-pressure continuous-flow conditions.^[99, 111] For example, esterifications, transesterifications, and direct carboxylic acid to nitrile reactions were performed applying supercritical ethanol, methanol, and acetonitrile with high yields. The reactor was resistively heated and it was capable of delivering temperatures up to 400 °C and pressures up to 200 bar.^[112]

Achieving high pressures in a safe and strictly controlled manner allows the application of superheated solvents. For example, in the prexasertib monolactate synthesis mentioned previously (p. 10), the formation of the pyrazole ring requires high-temperature conditions, where solvents with high boiling points would lead to isolation and purification issues.^[97] Utilizing CF methodology, pressurized tetrahydrofuran was applied at 130 °C, achieving superheated conditions and improved reaction rates with simpler product isolation.

2.2.3 Continuous-flow multi-step transformations

Performing multi-step transformations in CF greatly simplifies the synthesis process. The often circumstantial quenching, work-up, and purification steps between each reaction become unnecessary, thus the product of one reaction mixture becomes reactant as it travels from one reactor to another (Figure 5). Therefore, uninterrupted telescoped CF syntheses may save notable cost and time, which makes them attractive for the pharmaceutical industry.^[10, 113]

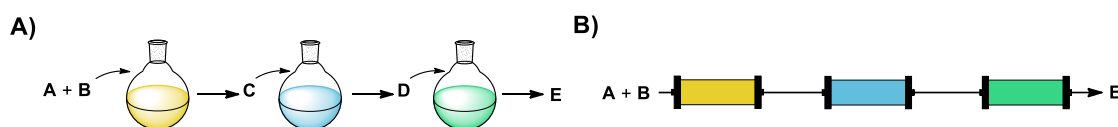


Figure 5. Classical segmented (A) and continuous-flow (B) multistep synthesis strategies

However, developing a multi-step CF synthesis does not mean the simple assembly of individual reactors, but creates several challenges and traps.^[11, 114, 115] There are critical parameters, which must be investigated accurately during the construction of a telescoped process, such as solvent, reactants, and residence time.

In recent years, CF systems became more and more sophisticated, involving complex synthetic solutions. There are several prominent examples for multi-step CF transformations. For instance, Jamison et al. developed a CF total synthesis of the anticonvulsant rufinamide.^[116] The reaction sequence involved an organic azide intermediate to form the essential triazole moiety of the compound. The azide generated *in situ* was not isolated but transformed immediately to the triazole ring *in continuo*.

Kobayashi and co-workers presented a gram-scale CF synthesis of both enantiomers of rolipram, an anti-inflammatory drug (Figure 6).^[117]

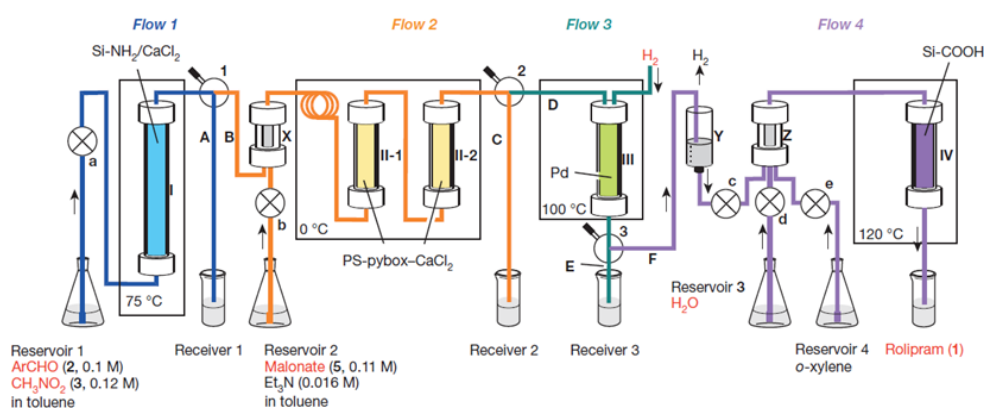


Figure 6. Diagram of the CF reactor system for the synthesis of (R)- and (S)-rolipram^[117]

During the eight reaction steps, only heterogeneous catalysts were used without the isolation of the intermediates or separation of any reagents or reactants. During the stability tests, the system proved to be stable under continuous processing for at least one week.

A reconfigurable CF system for the on-demand production of diphenhydramine hydrochloride, lidocaine hydrochloride, diazepam, and fluoxetine hydrochloride was reported by Adamo et al.^[118] They constructed a refrigerator-size CF equipment, fulfilling U.S. Pharmacopoeia standards with respect to product quality. Admirably, all downstream processes, such as crystallization, filtration, and formulation were integrated in the CF process. The productivity of each API was between 15–56 grams/day.

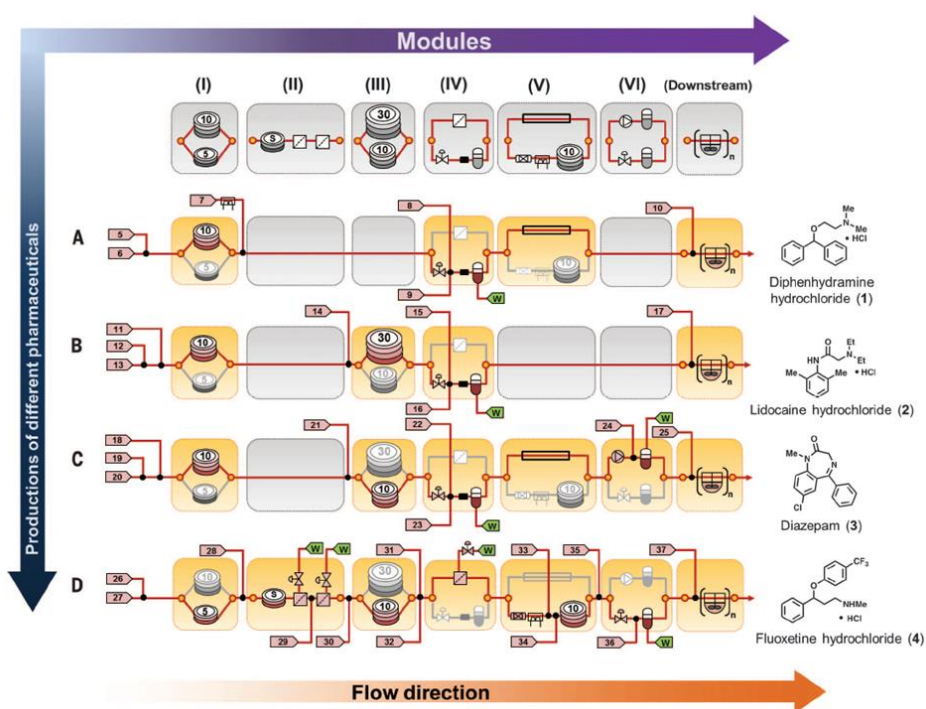


Figure 7. Schematic representation of a compact CF equipment for the synthesis of four different APIs^[118]

3. EXPERIMENTAL SECTION

3.1 General Information

Reagents and materials were commercially available and used as received. Analytical thin-layer chromatography was performed on Merck silica gel 60 F254 plates and flash column chromatography on Merck silica gel 60. Compounds were visualized by means of UV or KMnO_4 . NMR spectra were recorded on a Bruker Avance DRX 400 or 500 spectrometers, in CDCl_3 as solvent, with TMS as internal standard. ^1H spectra were recorded at 400.1 or 500.1 MHz, ^{13}C at 100.6 or 125.0 MHz. GC-MS analyses were carried out with a Thermofisher Scientific DSQ II Single Quadrupole GC/MS, on a 30 m \times 0.25 mm \times 0.25 μm TG-5SILMS capillary column (Thermo Scientific). The measurement parameters were as follows: column oven temperature: 30 $^\circ\text{C}$ (0–2 min), 30 to 250 $^\circ\text{C}$ at 10 $^\circ\text{C min}^{-1}$ (2–24 min), and 250 $^\circ\text{C}$ (24–26 min); injection temperature: 240 $^\circ\text{C}$; ion source temperature: 200 $^\circ\text{C}$; EI: 70 eV; carrier gas: He, at 1.5 mL min^{-1} ; injection volume: 2 μl ; split ratio: 1:50; and mass range: 50–500 m/z.

3.2 General Procedure for the Flow Reactions

3.2.1 Reactions with copper powder as catalytic source

Reactions were carried out in home-made flow reactors consisting of an HPLC pump (JASCO PU-880), stainless steel HPLC columns as catalyst bed (internal dimensions: 4.6 \times 50 mm, 4.63 \times 100 mm or 4.6 \times 150 mm), a stainless steel preheating coil (internal diameter 254 or 762 μm), and a commercially available backpressure regulator (IDEX P-455 BPR Assembly 750/1000 or Vici Jour JR-BPR2). The parts of the system were connected with stainless steel and PEEK capillary tubing (internal diameter 254 or 762 μm). The column was charged with copper powder (<425 μm particle size, 2 or 3.5 g depending on the length of the column) purchased from Sigma Aldrich and was sealed with compatible frits (2 mm pore size). The filled catalyst bed and the preheating coil were immersed in a heated oil bath.

3.2.2 Reactions with copper salts as catalytic source

Reactions were carried out in “home-made” flow reactors consisting of HPLC pumps (JASCO PU-880 and Knauer AZURA P 2.1 S), stainless steel coils as the active reactor zone (internal diameter: 760 μm , length: 7.5, 30.5 or 38.5 m), and a commercially available

70-bar BPR (IDEX P-455 BPR Assembly 1000, PEEK). The parts of the system were connected with stainless steel and PEEK capillary tubing (254 or 762 μm internal diameter). The stainless steel coil and the preheating coil were immersed in a heated oil bath.

3.3 Determination of residence times

To determine the residence time in a column reactor, the active reactor zone, a solution of a dye was pumped through the filled catalyst column. The elapsed time between the first contact of the dye with the cartridge/coil and the moment when the colored solution appeared at the outlet was measured. In the case of reactor coils, the residence time was calculated from the coil volume and flow rate.

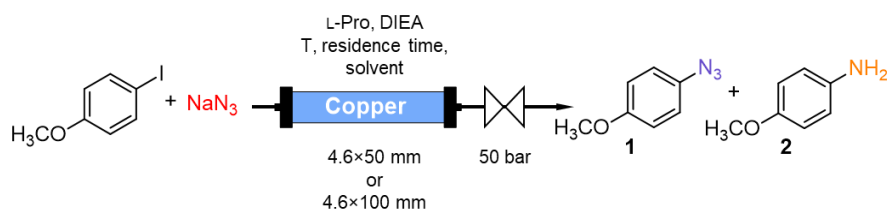
4. RESULTS AND DISCUSSION

4.1 Controlled transformations of aryl halides

As detailed in the Literature Survey *Section 2.1.1*, the copper-mediated nitrogenation of aryl halides with sodium azide can result in the formation of both aryl azides and anilines, where the selectivity is highly dependent on the reaction conditions. Exploiting the precise parameter control offered by the continuous-flow technology, we aimed to investigate the possibilities of the selective synthesis of both valuable products and develop a diversity-oriented CF synthesis method for the controlled transformations of aryl halides, gaining aryl azides or anilines by means of changing only the temperature and residence time.

4.1.1 Optimization

For the initial optimization study, the copper-catalyzed reaction of 4-iodoanisole with sodium azide was chosen as model reaction. According to literature data, L-proline and *N,N*-diisopropylethylamine (DIEA) were applied as ligand and base, respectively.^[40, 42, 43, 46, 119] As the active reactor zone, stainless steel columns loaded with copper powder was applied (internal dimensions: 4.6×50 mm or 4.6×100 mm). The catalyst bed was immersed into an oil bath for heating purposes and a 50-bar backpressure regulator was also installed (Scheme 8).



Scheme 8. Model reaction for the optimization of the copper-catalyzed nitrogenation reactions

Due to the narrow channels of the flow reactor, only clean solutions can be pumped through the system to prevent clogging. Because of the wide solubility properties of the starting materials (i.e., the haloarene, NaN₃, L-proline, and DIEA), a preliminary solvent compatibility test was carried out. As a result, solvent mixtures MeCN/H₂O 3:1, EtOH/H₂O 7:3, and DMSO/H₂O 4:1 proved to be convenient. The volume of the reaction mixture was 5 mL, where the concentration of the haloarene was 0.1 M along with 2 equiv. of NaN₃, 30 mol% L-proline and 30 mol% DIEA. The effects of the solvent systems were investigated in a reactor applying a 50-mm long stainless steel column loaded with 2 g of copper powder. The reaction conditions were 120 °C, 50 bar, and 7 min residence time (0.1 mL min⁻¹ flow

rate). As Figure 8 indicates, each solvent mixture had effect on both conversion and selectivity. In the case of MeCN/H₂O and EtOH/H₂O, low conversion rates were registered (below 40%) with high azide selectivity. The DMSO/H₂O system resulted in almost full conversion of the starting compound with a moderate azide/amine ratio of 71/29. Since our aim was to develop a synthesis method in which two different products can be synthesized from the same starting materials, DMSO/H₂O 4:1 was an ideal choice as reaction medium.

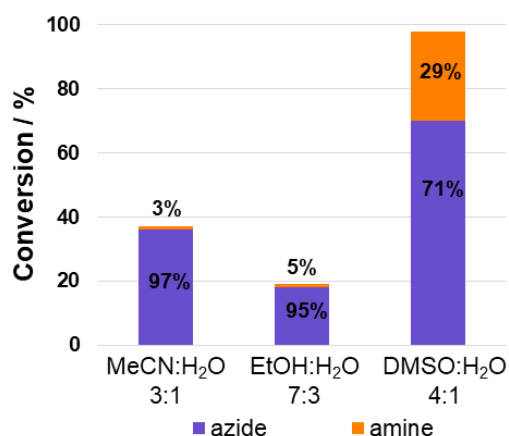


Figure 8. Effect of the solvent on the CF nitrogeneration of 4-iodoanisole (Scheme 8). (Product selectivity is marked with purple/orange column components.)

Elevation of the temperature had significant effects on conversion and chemoselectivity. From 75 °C to 120 °C, a significant increase in conversion occurred (from 47% to 98%; Figure 9). Lower temperatures favored azide formation (e.g., 100% azide selectivity was registered at 75 °C). Above 120 °C, a plateau in the selectivity was reached: at both 120 and 150 °C, the azide/amine ratio remained around 70:30.

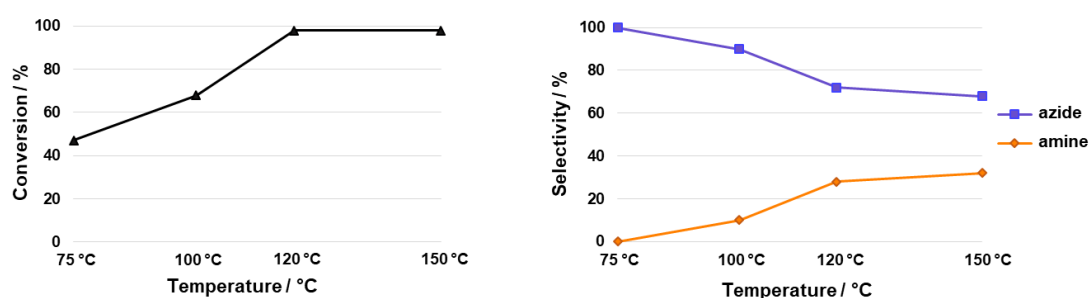


Figure 9. The effect of temperature in the 4-iodoanisole–NaN₃ model reaction (Scheme 8) using a 4.6×50 mm copper column as catalytic source. Conditions: 1 equiv. 4-iodoanisole (*c*=0.1 M), 2 equiv. NaN₃, 30 mol% L-proline, 30 mol% DIEA, DMSO/H₂O 4:1 as solvent, 50 bar, 0.1 mL min⁻¹ flow rate (7 min residence time)

Next, the effects of both NaN_3 and the auxiliaries were examined under the previously described conditions. The absence of the proline ligand led to poor conversion even at elevated temperature with 50% selectivity. (Table 1 entry 2). This led to the conclusion that the presence of the ligand is essential for the reaction. Interestingly, DIEA did not affect either the conversion or the selectivity (entry 3); therefore, in the remaining reactions the base was omitted. Reducing the amount of L-proline to 15 mol% resulted in a decrease in conversion (entry 4). However, we were delighted to find that the excess of NaN_3 could be reduced to 1.5 equiv. without any loss in conversion (entry 5).

Table 1. The effect of auxiliaries in the 4-iodoanisole– NaN_3 model reaction (Scheme 8) using a 4.6×50 mm copper column as catalytic source.^a

Entry	L-Pro (mol%)	DIEA (mol%)	NaN_3 (equiv.)	Conv. ^a (%)	Azide/amine ratio ^b
1	30	30	2	98	71:29
2 ^c	0	30	2	9	50:50
3	30	0	2	94	70:30
4	15	0	2	72	72:28
5	30	0	1.5	92	74:26

^a Conditions: 1 equiv. 4-iodoanisole ($c=0.1$ M), DMSO/ H_2O 4:1 as solvent, 120 °C, 50 bar, 0.1 mL min^{-1} flow rate (7 min residence time). ^b Determined by ^1H NMR spectroscopy of the crude material. ^c 150 °C reaction temperature.

Based on the above findings, the investigation of different flow rates was carried out using 1.5 equiv. of NaN_3 and in the absence of DIEA. The residence time was proved to have a crucial effect on both conversion and product selectivity, and showed interesting results at different temperatures (Figure 10). Although, a change in residence time from 25 to 3.5 min led to a sharp decrease in conversion at 120 °C, it did not affect the azide/amine ratio significantly (70:30 and 83:17, respectively). On the other hand, after elevating the temperature to 150 °C, the product selectivity could simply be inverted with the residence time: 79% amine at 25 min residence time, whereas 78% azide at 3.5 min residence time. The conversion rates were staying above 85% in each case.

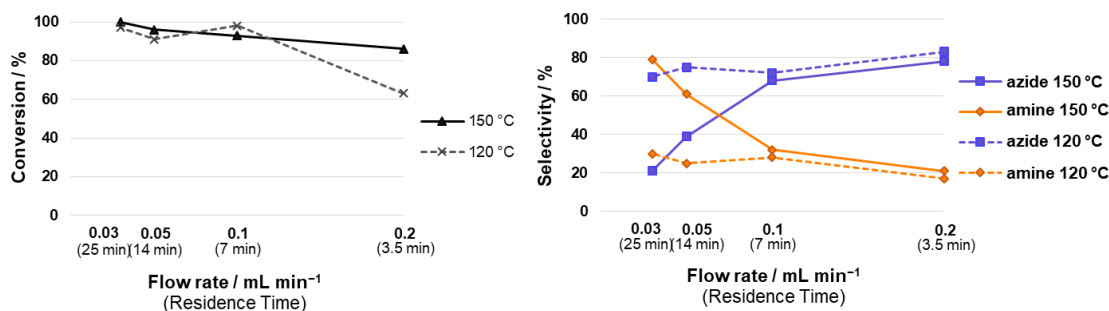


Figure 10. The effect of residence time in the 4-iodoanisole– NaN_3 model reaction (Scheme 8) using a 4.6×50 mm copper column as catalytic source. Conditions: 1 equiv. 4-iodoanisole ($c=0.1$ M), 1.5 equiv. NaN_3 , 30 mol% L-proline, DMSO/ H_2O 4:1 as solvent, 120 or 150 °C, 50 bar

These findings show that the product selectivity could easily be modified through fine-tuning the residence time and temperature. This encouraged us to achieve a more detailed picture on the effect of these parameters. However, beyond a certain limit, the residence time cannot be modified by the flow rate, thus the volume of the catalytic bed needs to be increased. A longer copper column was therefore selected as catalytic source (4.6×100 mm stainless steel column loaded with 3.5 g of copper powder) and the temperature dependence was next explored at 10.5 min residence time (0.1 mL min⁻¹ flow rate). As shown in Figure 11, elevating the temperature from 75 °C to 150 °C afforded a notable increase in conversion from 55 to 95%. Although these results are similar to those observed in the case of the shorter column (Figure 9), we found higher selectivities towards azide formation in the 75–120 °C temperature range. The best result was found at 100 °C with a conversion of 83% and an azide/amine ratio of 94:6.

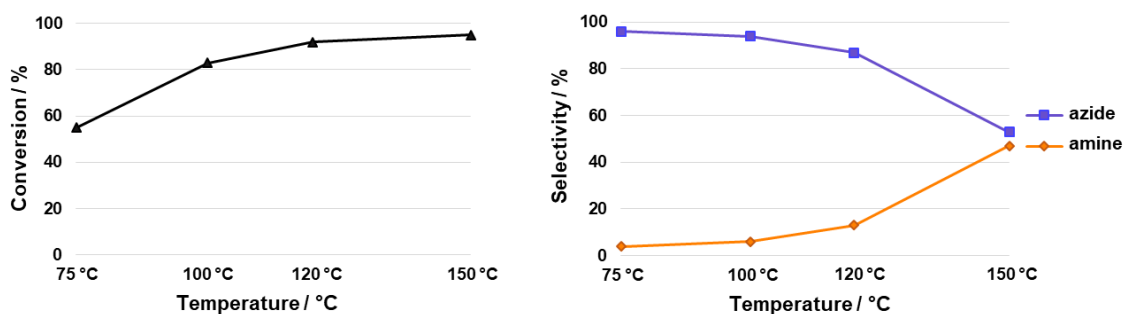


Figure 11. The effect of temperature in the 4-iodoanisole–NaN₃ model reaction (Scheme 8) using a 4.6×100 mm copper column as catalytic source. Conditions: 1 equiv. 4-iodoanisole (*c*=0.1 M), 1.5 equiv. NaN₃, 30 mol% *L*-proline, DMSO/H₂O 4:1 as solvent, 50 bar, 0.1 mL min⁻¹ flow rate (10.5 min residence time)

In order to achieve the selective synthesis of the corresponding amine product as well, we investigated the effect of the residence time. Since the highest amine ratio was achieved at 150 °C with 47% selectivity (Figure 11), reactions were carried out at a fixed temperature of 150 °C (Figure 12). Gratifyingly, the amount of azide **1** decreased strongly with increasing residence times. Amine **2** was formed with an outstanding selectivity of 98% at 100% conversion using a residence time of 35 min (equal to 0.03 mL min⁻¹ flow rate).

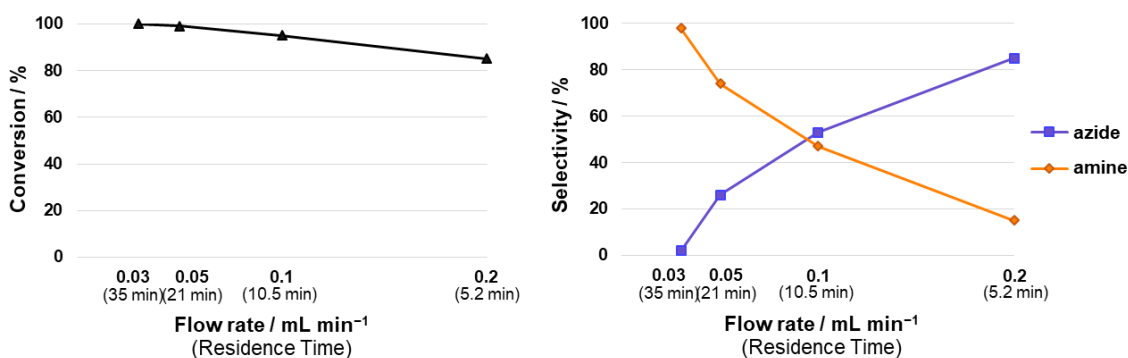


Figure 12. The effect of residence time in the 4-iodoanisole–NaN₃ model reaction (Scheme 8) using a 4.6×100 mm copper column as catalytic source. Conditions: 1 equiv. 4-iodoanisole (c=0.1 M), 1.5 equiv. NaN₃, 30 mol% L-proline, DMSO/H₂O 4:1 as solvent, 150 °C, 50 bar

At the end of the optimization phase, we had two distinct parameter sets in hand for the selective synthesis of either azide **1** or amine **2** using 4-iodoanisole as common starting material (Figure 13). The product selectivity of the azide compound was 94% with an 83% conversion at 100 °C and 10.5 min residence time, while the amine product was collected at higher temperature and residence time (150 °C and 35 min, respectively) with complete conversion and 98% selectivity. Such precise control over the reaction parameters is not available in conventional batch reactions, which may explain the inconsistency of earlier literature observations.

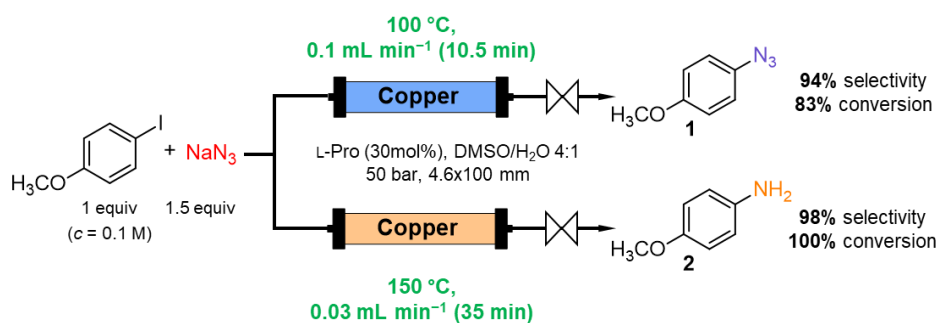


Figure 13. Optimal reaction parameters for the diversity-oriented synthesis of 1-azido-4-methoxybenzene (**1**) and 4-methoxyaniline (**2**) from 4-iodoanisole as starting material

To gain mechanistic insights, the thermal stability of the preformed azide **1** was next investigated. It is known that after copper-mediated azidation, subsequent azide reduction/decomposition is of crucial importance in terms of product selectivity.^[42-44] However, the nature of this step is still ambiguous. The thermal decomposition of azides has been known from the literature for a long time,^[120, 121] and there are examples for copper-mediated azide decomposition/reduction.^[122, 123] Moreover, there are reports in which azide anions are suggested to operate as the reducing agent.^[43] When the solution of the preformed azide was pumped through an inert column packed with quartz sand at temperature and

residence time utilized earlier for the amine synthesis (150 °C and 35 min), no decomposition was detected in the absence of ligand and NaN₃ (Table 2, entry 1). However, when the experiment was repeated in the presence of NaN₃, significant amine formation occurred (52:48 azide/amine ratio; entry 2). When the reaction was performed on a copper column, the azide completely transformed to the corresponding amine (entry 3). At 75 °C, amine formation decreased to 16% (entry 4), which elevated to 30% in the presence of L-proline (entry 5). On the basis of these observations, the azide–amine transformation is not a purely thermal process: it is strongly dependent on both the catalyst and also on the auxiliaries present.

Table 2. Investigation of the nature of the azide–amine transformation in the case of 1-azido-4-methoxybenzene in a continuous-flow reactor

Entry	Column packing	L-Pro (mol%)	NaN ₃ (equiv.)	Azide/amine ratio ^a
1	Quartz sand	-	-	100:0
2	Quartz sand	-	1.5	52:48
3	Copper powder	-	-	0:100
4 ^b	Copper powder	-	-	84:16
5 ^b	Copper powder	30	-	70:30

^a Determined by ¹H NMR spectroscopy of the crude material. ^b 75 °C temperature.

4.1.2 Synthesis of aryl amines and aryl azides

After defining the optimal parameter sets, the scope and the limits of the methodology were next explored. The conditions for the aryl amine synthesis proved to be widely tolerant to diversely substituted aryl iodides. Both electron-donating and electron-withdrawing substituents were nicely tolerated, and anilines **2-9** were formed in high conversion (94–100%) and with excellent chemoselectivity (Table 3, entries 1–8). Aryl bromides were also investigated (entries 9–14). Both *para*- and *meta*-substituted compounds gave excellent selectivities (89–100%) and high conversions similar to those of iodo derivatives (entries 9, 10, and 13). As expected, *ortho*-substituted aryl bromides (entries 11, 12, 14) were less reactive, possibly due to steric hindrance. It is important to point out that the flow methodology nicely tolerated various aryl halides decorated with readily convertible functional groups (see entries 8, 12, 13, and 14). This is of high importance as concerns further transformations of the anilines obtained.

Table 3. Continuous-flow synthesis of various aryl amines from aryl halides as starting materials

Entry	Starting material	Product	Conv. ^a (%)	Select. ^a (%)
1			100	98
2			94	100
3			100	100
4			100	100
5			100	100
6			100	95
7			98	100
8			100	100
9			91	89
10			100	100
11			60	100
12			88	100
13			100	90
14			81	100

^a Determined by ¹H NMR spectroscopy of the crude material.

The selective aryl azide synthesis proved more challenging, due to the sensitivity of the azide reduction/decomposition. Temperature and residence time optimized previously (100 °C and 10.5 min) had to be modified for each substrate to obtain satisfactory conversions and selectivities (Table 4). Interestingly, minor differences in the substitution pattern of the

haloarene led to notable changes in the reaction outcome. For instance, under the conditions applied earlier for 4-iodoanisole, 1-iodo-4-methylbenzene and 1-iodo-4-ethylbenzene were transformed to the corresponding azides with low selectivities of 11 and 36%, respectively (see entries 2 and 6 vs. entry 1). To our delight, elevating the reaction temperature from 100 to 120 °C and reducing the residence time to 5.2 min boosted the azide selectivity to 90 and 82%, respectively, while maintaining high conversions (entries 3–4 and 7).

Similarly, in the case of 1-(*tert*-butyl)-4-iodobenzene, a temperature increase and residence time decrease were necessary to increase the conversion to 90%, while maintaining a good azide selectivity (entries 8–12). Good conversion and high azide selectivity were also reached at 80 °C by using a residence time of 21 min (entry 13). Interestingly, increasing the residence time in the 4-iodoaniline–NaN₃ reaction from 10.5 to 21 min at 100 °C had no effects on the azide selectivity, but improved the conversion from 62% to a decent level of 86% (entries 14 and 15).

Table 4. Continuous-flow synthesis of various aryl azides from aryl halides as starting materials

Entry	Starting material	Product	Conditions	Conv. ^a (%)	Select. ^a (%)
1			100 °C, 0.1 mL min ⁻¹ (10.5 min)	83	94
2			100 °C, 0.1 mL min ⁻¹ (10.5 min)	89	11
3			120 °C, 0.15 mL min ⁻¹ (7.8 min)	87	65
4			120 °C, 0.2 mL min ⁻¹ (5.2 min)	78	90
5			140 °C, 0.15 mL min ⁻¹ (7.8 min)	96	16
6			100 °C, 0.1 mL min ⁻¹ (10.5 min)	70	36
7			120 °C, 0.2 mL min ⁻¹ (5.2 min)	82	82
8			100 °C, 0.1 mL min ⁻¹ (10.5 min)	77	79
9			100 °C, 0.15 mL min ⁻¹ (7.8 min)	65	80
10			120 °C, 0.2 mL min ⁻¹ (5.2 min)	90	71
11			120 °C, 0.25 mL min ⁻¹ (4 min)	71	85
12			140 °C, 0.25 mL min ⁻¹ (4 min)	88	61
13			80 °C, 0.05 mL min ⁻¹ (21 min)	80	75
14 ^{b)}			100 °C, 0.1 mL min ⁻¹ (10.5 min)	62	100
15 ^{b)}			100 °C, 0.05 mL min ⁻¹ (21 min)	86	100

^a Determined by ¹H NMR spectroscopy of the crude material. ^b Due to solubility issues DMSO/H₂O 5:1 was used as solvent.

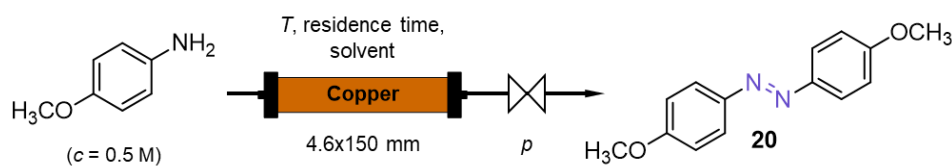
4.2 New parameter spaces for the oxidative homocoupling of aniline derivatives

4.2.1 Reactions mediated by copper powder

4.2.1.1 Optimization of reaction conditions

As detailed in *Section 2.1.2*, aromatic azo compounds are members of a complex redox system, where the balance between the species has a significant thermal dependence. However, conventional batch equipments provide wide temperature profiles, where uneven heat distribution may easily lead to hot-spot formation promoting side-reactions, lowering the selectivity and the yield.^[106] Therefore, we envisioned to develop a continuous-flow synthesis method for the copper-catalyzed oxidative homocoupling of arylamines, which allows to overcome the restraints of the batch-type processes, and provides novel process windows and increased parameter space for chemical synthesis.

As a simple source of catalytically active species, copper powder was chosen and charged into a stainless steel cylindrical column. As model reaction for the optimization study, the oxidative homocoupling of *p*-anisidine was chosen (Scheme 9).



Scheme 9. Model reaction for optimization of the copper-catalyzed oxidative homocoupling

To avoid precipitation and blockage in the reactor channels, the applied concentration of the starting material proved to be 0.5 M. According to literature data, due to the typical temperature range 60–100 °C, the reaction media are mainly nonvolatile solvents, such as toluene^[69, 72, 75] and MeCN.^[69, 71-75] As a consequence of the restrictive batch technology, the application of low-boiling solvents is still unexplored in this transformation. Thus we envisioned to investigate the performance of various volatile solvents under pressurized and high-temperature conditions. The solvent dependence of the model reaction was performed at 100 °C, 50 bar, and 18 min residence time (0.1 mL min⁻¹ flow rate) in the presence of pyridine, as base. Interestingly, in the case of toluene and MeCN, only poor conversions were registered with the value of 12% and 4% respectively (Table 5 entries 1 and 2). Conversions in EtOH and H₂O could not be evaluated due to solubility issues (entries 3 and 4). Although among low-boiling point solvents, acetone provided only trace amounts of the product (entry 5), the utilization of dichloromethane led to an impressive conversion of 52% (entry 6). Since CH₂Cl₂ is known to be the most acceptable among chlorinated

solvents in terms of safety and environmental impacts,^[124] the use of further halogenated solvents was not explored.

Table 5. Investigation of the solvent dependence of the oxidative homocoupling of *p*-anisidine under continuous-flow conditions (Scheme 9)^a

Entry	Solvent	Conv. ^b (%)
1	toluene	12
2	MeCN	4
3	EtOH	n.d. ^c
4	water	n.d. ^c
5	acetone	trace
6	CH ₂ Cl ₂	52

^a Reactions were carried out with 1 equiv. of *p*-anisidine (*c*=0.5 M) and 2 equiv. of pyridine as base in the specified solvent at 100 °C, 50 bar and 0.1 mL min⁻¹ flow rate. ^b Determined by ¹H NMR spectroscopic analysis of the crude product. Chemoselectivity of the homocoupling was 100% in all reactions. ^c Not determined.

Next, the effects of various nitrogen bases on the model reaction were investigated. In the absence of base, no reaction was observed (Table 6, entry 1), which is consistent with literature data, that is, the base has an evident role in both the activation of copper and a subsequent oxidation step.^[72] Switching pyridine to any other base resulted in a decrease in conversion: triethylamine (TEA) and DIEA led to 41% and 12%, respectively (entry 3 and 4), while *N*-methylmorpholine and imidazole gave only trace amounts of the corresponding azobenzene (entry 5 and 6). Notably, the chemoselectivity of the reactions was 100% in all cases.

Table 6. Investigation of the effects of various nitrogen bases on the oxidative homocoupling of *p*-anisidine under continuous-flow conditions (Scheme 9)^a

Entry	Base	Conv. ^b (%)
1	no base	0
2	pyridine	52
3	TEA	41
4	DIEA	12
5	<i>N</i> -methylmorpholine	trace
6	imidazole	trace

^a Reactions were carried out by using 1 equiv. of *p*-anisidine (*c*=0.5 M) and 2 equiv. of base in CH₂Cl₂ at 100 °C, 50 bar and 0.1 mL min⁻¹ flow rate. ^b Determined by ¹H NMR spectroscopic analysis of the crude product. Chemoselectivity of the homocoupling was 100% in all reactions.

Although pressurizing had no significant effects on conversion in the 10–100 bar range, 50 bar pressure was chosen as an optimal value to prevent solvent boil-over. On the other hand, raising the temperature from 100 to 120 °C had a dramatic effect on conversion with

an increase from 52 to 100% (Figure 14 A). This phenomenon indicates an energy barrier between 100 and 120 °C, which could be overcome by means of the application of overheated CH₂Cl₂, as a novel parameter space in this reaction. Investigating the effect of the flow rate led to an optimal value of 0.1 mL min⁻¹ (18 min residence time), since an increase to 0.2 mL min⁻¹ (9 min) resulted in a significant conversion drop to 37% (Figure 14 B).

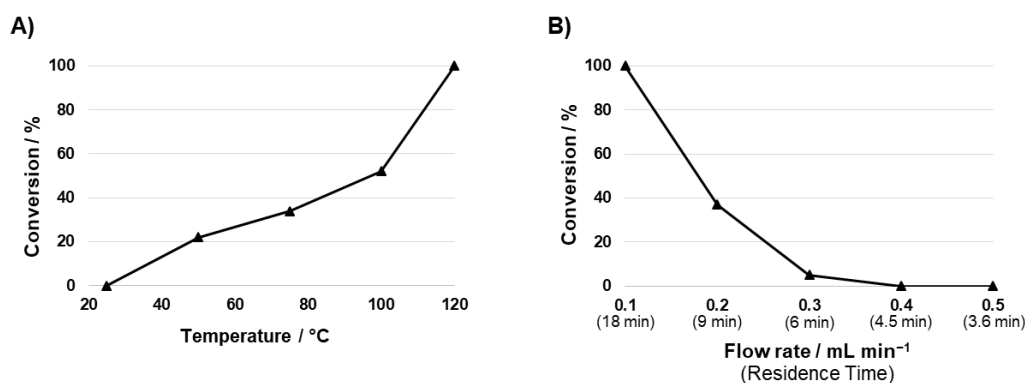


Figure 14. Investigation of the temperature dependence (A) and the flow rate dependence of the oxidative homocoupling of *p*-anisidine in continuous-flow mode. Reaction conditions: A) 50 bar, flow rate 0.1 mL min⁻¹, 1 equiv. of *p*-anisidine (*c* = 0.5 M), 2 equiv. of pyridine as base, in CH₂Cl₂ as solvent. B): 50 bar, 120 °C, 1 equiv. of *p*-anisidine (*c* = 0.5 M), 2 equiv. of pyridine as base, in CH₂Cl₂ as solvent (The residence times corresponding to the flow rates are given in parentheses.)

In the last step of the optimization process, the amount of the pyridine base was successfully decreased to one equiv. without any drop in the conversion (Table 7, entries 1 and 2). Herewith, we achieved the optimal conditions for the model reaction of oxidative homocoupling. 120 °C temperature at 18 min residence time was essential to conquer the energy barrier of the reaction and maintain a sufficient catalyst–substrate contact time. The safe utilization of pressure allowed the operation of volatile CH₂Cl₂ at temperatures far above its boiling point, leading to an unexplored chemical parameter space for the homocoupling reaction.

Table 7. Investigation of the effects of various pyridine amounts on the oxidative homocoupling of *p*-anisidine under continuous-flow conditions^a

Entry	Pyridine [equiv.]	Conv. ^b (%)
1	2	100
2	1	100
3	0.75	35
4	0.5	34

^a Reactions were carried out with 1 equiv. of *p*-anisidine (*c*=0.5 M) and a specified amount of pyridine as base in CH₂Cl₂ at 120 °C, 50 bar and 0.1 mL min⁻¹ flow rate.

^b Determined by ¹H NMR spectroscopic analysis of the crude product. Chemoselectivity of the homocoupling was 100% in all cases.

4.2.1.2 Scope and scale-up experiments

The reactivity of various aniline derivatives was investigated under the previously optimized conditions (Table 8). The results allowed us to explore the reactivity patterns of different substituents. Similar to *p*-anisidine, highly acceptable results were obtained with 4-ethoxyaniline and aniline achieving complete conversions and excellent yields of 93–97% (entries 1–3). Anilines bearing alkyl groups were nicely tolerated irrespective of the position of the substituent (entries 4–7), and even anilines containing bulky moieties, such as isopropyl, phenoxy and dimethylamino groups, were converted quantitatively to the desired product with isolated yields of 88–97% (entries 8–10). The syntheses of multisubstituted aromatic azo compounds are quite rare in the literature, possibly because of the exceptional steric hindrance generated by the functional groups.^[63, 64, 73] We were delighted to find that di- and trisubstituted aniline derivatives showed excellent reactivities. Even di-*ortho*-substituted anilines were converted quantitatively to the desired adducts (entries 12 and 13), and all corresponding multisubstituted derivatives were achieved in excellent yields of 89–93% (entries 11–14). Gratifyingly, full chemoselectivity was registered in each reaction.

Table 8. Exploring the reactivity of various aniline derivatives in oxidative homocoupling^a

Entry	Product	Conv. ^b (%)	Entry	Product	Conv. ^b (%)
1		100 (96) ^c	8		100 (97) ^c
2		100 (97) ^c	9		100 (92) ^c
3		100 (93) ^c	10		100 (88) ^c
4		95 (91) ^c	11		100 (90) ^c
5		100 (97) ^c	12		100 (89) ^c
6		100 (97) ^c	13		100 (93) ^c
7		100 (95) ^c	14		100 (91) ^c

Aniline starting materials are not shown. ^a Reactions were carried out with 1 equiv. of arylamine (*c*=0.5 M) and 1 equiv. of pyridine as base in CH₂Cl₂ at 120 °C, 50 bar and 0.1 mL min⁻¹ flow rate. ^b Determined by ¹H NMR spectroscopic analysis of the crude product. Chemoselectivity of the homocoupling was 100% in all reactions. ^c Isolated yields indicated in parentheses.

Arylamines with electron-withdrawing moieties are significantly less reactive in oxidative coupling reactions as a consequence of the reduced nucleophilicity of the amine group.^[72] Therefore, the reactivity of halogen-substituted aniline derivatives was studied (Table 9). According to preliminary investigations, the amount of the pyridine base was raised to 2 equiv. 4-Chloroaniline showed a conversion of 66% under the conditions of 120 °C, 50 bar, and 0.1 mL min⁻¹ flow rate (entry 1), and the rate of the reaction decreased significantly upon changing to the *meta*- and then to the *ortho*-substituted derivatives, with conversions of merely 58% and 4% in the case of 3- and 2-chloroaniline, respectively (entries 2 and 3). Considering the powerful temperature dependence described previously, the reactions of 4-, 3-, and 2-chloroaniline were repeated at 140 °C. This resulted in significant improvements in reaction rates: quantitative conversion and excellent yield of 90% in the case of 4-chloroaniline (entry 1), and conversions of 70% and 23% together with yields of 59% and 15% in the cases of 3- and 2-chloroaniline, respectively (entries 2 and 3). 2-Bromoaniline displayed lower reactivity, with no reaction at 120 °C, and merely 15% conversion at 140 °C (entry 4). Interestingly, the homocoupling of 3-chloro-4-methoxyaniline, containing both an electron-donating and an electron-withdrawing substituent, proceeded very well at 120 °C and gave quantitative conversion and an excellent yield of 93% in the presence of only 1 equiv. of pyridine base (entry 5).

Table 9. Investigation of the reactivity of halogen-substituted aniline derivatives in oxidative homocoupling at 120 and 140 °C^a

Entry	Product	Conversion (%) ^b	
		120 °C	140 °C
1	34	66	100 (90) ^d
2	35	58	70 (59) ^d
3	36	4	23 (15) ^d
4	37	0	15
5 ^c	38	100 (93) ^d	-

Aniline starting materials are not shown. ^a Reactions were carried out with 1 equiv. of arylamine (*c*=0.5 M) and 2 equiv. of pyridine as base in CH₂Cl₂ at 50 bar and 0.1 mL min⁻¹ flow rate. ^b Determined by ¹H NMR spectroscopic analysis of the crude product. Chemoselectivity of the homocoupling was 100% in all reactions. ^c 1 equiv. of pyridine was used as base. ^d Yield of the isolated product.

To probe the preparative capabilities of the continuous-flow process, the synthesis of 4,4'-dimethoxyazobenzene (Scheme 9) was scaled out simply as a function of the operation time. Reaction conditions optimized previously were applied (120 °C, 50 bar, 0.1 mL min⁻¹ flow rate, CH₂Cl₂ solvent) without any change in the *p*-anisidine or pyridine concentration (0.5 M each). A 30-fold scale-out was performed pumping 45 mL of the reaction mixture through the reactor in 7.5 h. In every 75 min a separate fraction of the continuously eluted product solution was collected. Quantitative conversion was detected in all portions, suggesting that there was no decrease in catalytic activity during the experiment. After a simple evaporation (pyridine could be evaporated off), 2.36 g of pure product was isolated, which corresponded to an overall yield of 86% and an excellent throughput of 0.32 g pure product per hour.

4.2.2 Cu(II)Fe(II)-layered double hydroxide, as solid base catalyst

4.2.2.1 Comparison of reactivity of the oxidative homocoupling of *p*-anisidine

As part of a cooperation, an opportunity was raised to investigate the catalytic activity of a copper-containing layered double hydroxide (LDH), namely Cu(II)Fe(III)-LDH in the oxidative homocoupling of anilines (Figure 15). LDHs are two-dimensional anionic clays with well-defined layered structures.^[125] The layers consist of di- and trivalent metal cations being octahedrally surrounded by hydroxide ions. LDHs with layers of catalytically active metals can act as highly active and selective solid catalysts.^[126] Although the use of as-prepared LDHs employed as bifunctional (basic character plus the redox activity of the framework metal ion) catalysts is scarce, we speculated that the Cu(II)Fe(III)-LDH material might act as a solid base and, at the same time, as a source for a catalytically active metal, thereby possibly eliminating the need for an extraneous base in the homocoupling reaction.

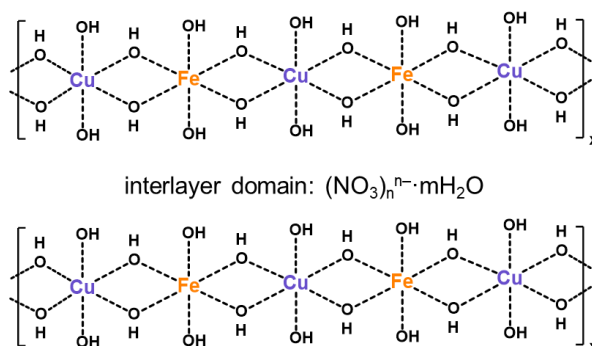
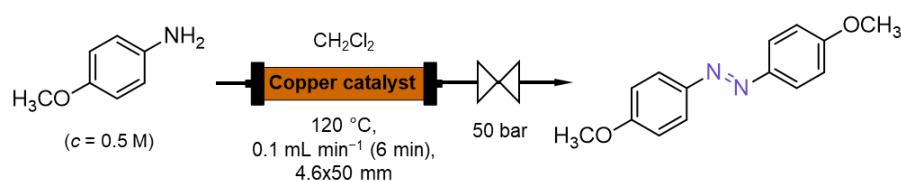


Figure 15. Schematic representation of the structure of Cu(II)Fe(III)-LDH

As described above, the utilization of copper powder as catalytic source necessitated the presence of pyridine as extraneous base (Table 6). This is in accordance with the pronounced role of the base in the final hydrazo–azo dehydrogenation step.^[72] In a series of preliminary experiments, the catalytic activity of the Cu(II)Fe(III)-LDH was investigated in the oxidative dimerization of *p*-anisidine and compared with the results gained with copper powder as catalytic source (Scheme 10). The copper catalysts were charged in a stainless steel column (4.6×50 mm) and the effect of the temperature was investigated in the presence of 1 equiv. of pyridine and in the absence of base. The residence time was 6 minutes in each case (0.1 mL min⁻¹ flow rate).



Scheme 10. Model reaction for the investigation of the effects of various copper sources and additives on the oxidative dimerization of *p*-anisidine

As shown in Figure 16 A, in the presence of 1 equiv. pyridine, higher conversions were registered in the case of the LDH than with Cu powder. Upon exploring the reactivities of the copper catalysts in the absence of pyridine (Figure 16 B), it became clear that the application of Cu(II)Fe(III)-LDH significantly boosts the rates of the oxidative homocoupling of *p*-anisidine. It promoted the reaction without any added base and the conversion reached a moderate value of 60% at 140 °C (0.1 mL min⁻¹ flow rate).

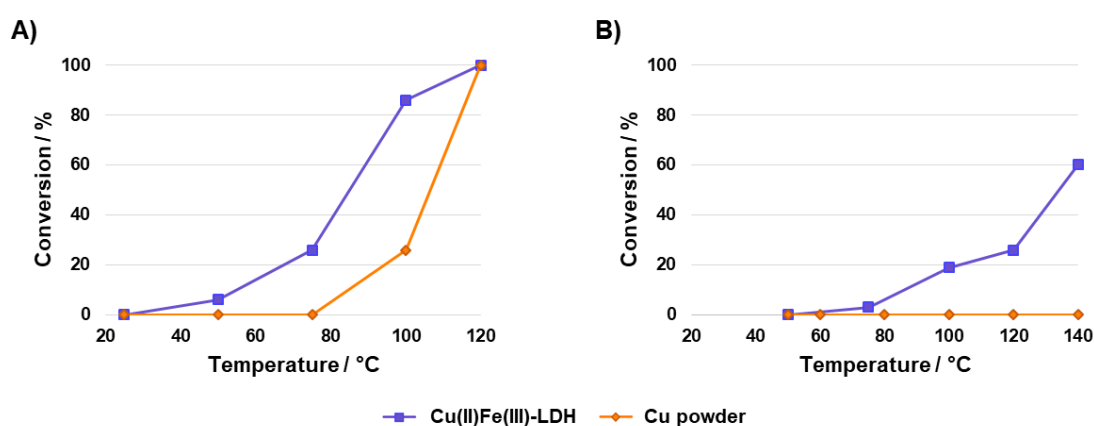


Figure 16. Investigating the effects of the temperature and different copper sources in the presence of 1 equiv. of pyridine (A) and in the absence of pyridine (B) in the case of the model reaction (Scheme 10)

In further experiments, the effect of the residence time at different temperatures was investigated (Figure 17). At 0.1 mL min⁻¹ flow rate (6 min residence time), 150 °C temperature was needed to reach full conversion. In contrast, at 0.03 mL min⁻¹ (20 min residence

time) complete transformation of the starting material was observed even at 130 °C. However, due to possible overreaction, traces of an azoxy side-product appeared in the reaction mixture, leading to a chemoselectivity drop to 94%. Applying 30 min residence time at 120 °C also led to azoxy-formation, resulting in 89% selectivity. To our delight, complete conversion and 100% selectivity were registered at 110 °C by using a residence time of 30 min.

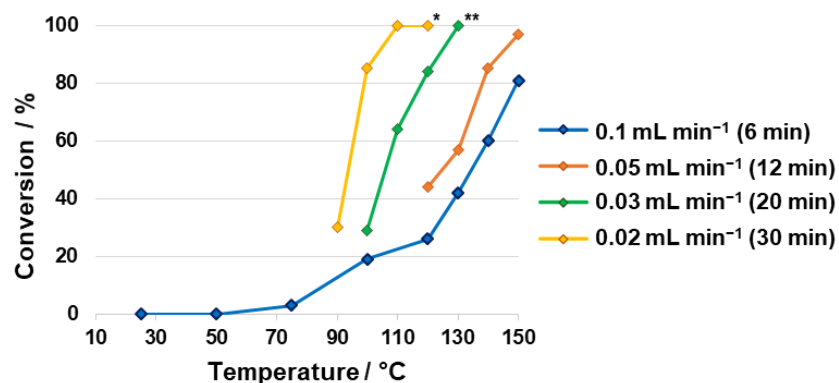


Figure 17. Investigation of the effects of the temperature and the residence time on the oxidative dimerization of *p*-anisidine (Scheme 10). *Selectivity was 89%. **Selectivity was 94%. Selectivity was 100% in each further point. (Residence time is given in parentheses.) Reaction conditions: 1 equiv. of *p*-anisidine ($c = 0.5 M$) in CH_2Cl_2 , at 50 bar

4.2.2.2 Scope and scale-out experiments

Next, the reactivity of the Cu(II)Fe(III)-LDH catalyst was investigated for the oxidative homocoupling of anilines with varied substitution patterns at the previously set conditions (110 °C, 30 min residence time, 50 bar). Gratifyingly, the homocoupling of methyl-, ethyl-, methoxy-, and ethoxy-substituted anilines furnished the products with high conversions and yields (Table 10, entries 1–7). Aromatic amines containing bulky moieties, such as isopropyl and dimethylamino, were also reacted in high yields (91 and 93%, entries 8 and 9). Moreover, di- and trisubstituted anilines were converted effectively to the corresponding azobenzene derivatives without the presence of any pyridine base (entries 10–12). Even 2,4,6-trimethylaniline, a di-*ortho*-substituted compound, was transformed in a yield of 96% (entry 10). It is important to emphasize, that no side-products were detected in any of the above reactions; that is, azobenzene products were obtained chemoselectively. It is also notable that in all reactions the *E* azobenzene isomer was isolated exclusively as corroborated by the ¹H NMR spectra of the crude products.

Table 10. Exploring the oxidative homocoupling of diversely substituted anilines applying Cu(II)Fe(III)-LDH as catalyst

Entry	Product	Conv. ^{a,b} (%)	Entry	Amine	Conv. ^{a,b} (%)
1		100 (96)	7		100 (95)
2		100 (97)	8		98 (91)
3		99 (93)	9		100 (93)
4		100 (98)	10		99 (96)
5		98 (95)	11		100 (92)
6		100 (97)	12		98 (94)

Aniline starting materials are not shown. ^a Determined by ¹H NMR. ^b Chemoselectivity of the azobenzene formation was 100% in all reactions. ^c Isolated yields indicated in parentheses.

Subsequently, the oxidative dimerization of the model reaction was scaled out in order to investigate the preparative capability and stability of the catalyst (Figure 18). To maximize the productivity of the synthesis and avoid any product precipitation and clogging in the reactor channels, the concentration of *p*-anisidine was decreased to 0.3 M and the residence time was reduced to 10 min (0.06 mL min⁻¹). Temperature and pressure remained as optimized earlier, namely 110 °C and 50 bar. In a 15-h reaction window, conversion and selectivity were determined in every hour to get a clear view of the actual catalyst activity. To our delight, the conversion was constant at around 70%. From the eleventh hour, a slow decrease in catalyst activity took place, but a conversion of 59% could still be detected at the end of the experiment after 15 h. In the large-scale synthesis, 1.28 g of 4,4'-dimethoxyazobenzene was isolated corresponding to an overall yield of 65%.

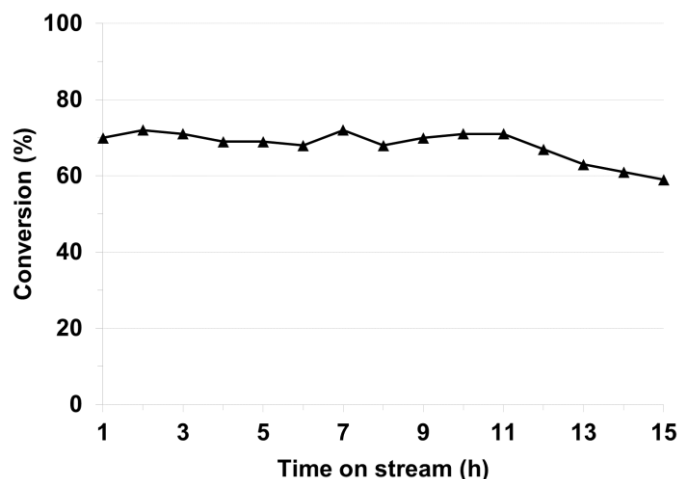


Figure 18. Investigating the large-scale synthetic capability of the Cu(II)Fe(III)-LDH catalyst in the model reaction (Scheme 10). Chemoselectivity of the azobenzene formation was 100% throughout the process

4.3 Multi-step synthesis of 3,5-disubstituted pyrazoles

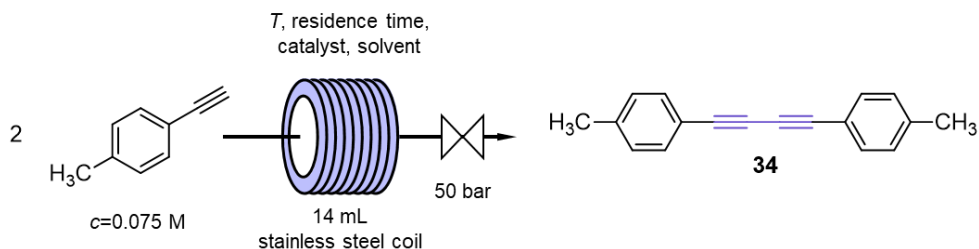
4.3.1 Step-by-step optimization

On the basis of the importance of pyrazoles and the drawbacks in their syntheses, we aimed to develop a practical two-step continuous-flow synthesis of 3,5-disubstituted pyrazoles. The planned reaction sequence incorporated two reactions: (i) a copper-catalyzed alkyne homocoupling and (ii) a Cope-type hydroamination of the 1,3-diyne with hydrazine and a cyclization thereafter. To avoid possible side-reactions facilitated by the presence of the catalytic metal during the second step, an in-line metal removing unit was installed after the first CF reactor. Therefore, a two-step telescoped process was developed.

To explore and optimize the critical reaction parameters, the two reactions were investigated separately in a step-by-step manner. After having the necessary knowledge and optimal reaction conditions in hand, a multistep telescoped sequence was constructed where the 1,3-diyne intermediate was transformed directly into the corresponding pyrazole.

For the optimization of the 1,3-diyne synthesis, the catalytic dimerization of 4-ethynyltoluene was chosen as model reaction (Scheme 11). Being considered that applying a soluble catalyst can create a robust and well-defined synthesis system and may avoid uncontrollable leaching problems, we chose homogeneous copper sources over solid catalysts. In order to avoid precipitation in either reaction step, detailed solvent compatibility tests were carried out investigating not only the copper catalyst and the solvent, but also the starting alkyne and the hydrazine monohydrate. According to literature data, various copper salts and complexes were investigated as possible catalysts. From several possible solvents,

DMSO and EtOH proved to be widely tolerant with all reactants. As a result of the investigation of the catalytic sources, $[\text{Cu}(\text{phen})(\text{PPh}_3)_2]\text{NO}_3$ and CuBr_2 proved to be suitable for our study (for detailed experimental results, see the ESI of the corresponding publication).



Scheme 11. Oxidative homocoupling of 4-ethynyltoluene in a continuous-flow reactor

The reactivity of the selected copper sources was investigated in the dimerization reaction of 4-ethynyltoluene (Table 11). A 14 mL stainless steel coil served as reactor and the initial conditions were as follows: 120 °C, 50 bar, and 0.2 mL min⁻¹ flow rate (70 min residence time). 0.075 M alkyne concentration proved to be optimal – higher concentrations led to precipitation. 0.06 equiv. of the copper catalyst was applied in DMSO or EtOH as solvent.

Applying $[\text{Cu}(\text{phen})(\text{PPh}_3)_2]\text{NO}_3$ as catalyst, no conversion was detected in either solvent even in the presence of 0.5 equiv. of DIEA as base (Table 11, entries 1–4).

Next, the catalytic activity of CuBr_2 was investigated. 0.5 equiv. of *N,N,N',N'*-tetramethylethylenediamine (TMEDA) and 0.5 equiv. of DIEA were added to the reaction mixture, serving as ligand and base, respectively. Gratifyingly, full conversion and selectivity were observed in DMSO (entry 6). The absence of the additives led to precipitation and clogging in the reactor channels.

Table 11. Investigation of the copper sources on the homocoupling of 4-ethynyltoluene. Conditions: 1 equiv. 4-ethynyltoluene ($c = 0.075 \text{ M}$), 6 mol% catalyst, 120 °C, 0.2 mL min⁻¹ (70 min residence time)

Entry	Catalyst	Additive ^a	Solvent	Conv. ^b
1	$[\text{Cu}(\text{phen})(\text{PPh}_3)_2]\text{NO}_3$	-	DMSO	0
2	$[\text{Cu}(\text{phen})(\text{PPh}_3)_2]\text{NO}_3$	-	EtOH	0
3	$[\text{Cu}(\text{phen})(\text{PPh}_3)_2]\text{NO}_3$	DIEA	DMSO	0
4	$[\text{Cu}(\text{phen})(\text{PPh}_3)_2]\text{NO}_3$	DIEA	EtOH	0
5	CuBr_2	-	DMSO	n.d. ^c
6	CuBr_2	TMEDA, DIEA	DMSO	100

^a 0.5 equiv. TMEDA, 0.5 equiv. DIEA. ^b Determined by ¹H NMR spectroscopy of the crude material. Chemoselectivity of diyne formation was 100% in all reactions. ^c No data, clogging occurred.

According to the results above, CuBr₂ was chosen as catalyst in the presence of TMEDA and DIEA. Subsequently, the effects of the residence time were investigated. To our delight, the initial 70 min residence time could successfully be reduced to 14 min (1 mL min⁻¹ flow rate) without any decrease in the conversion (Figure 19). A further decrease in the residence time led to a significant conversion drop (65% at 10.5 min residence time).

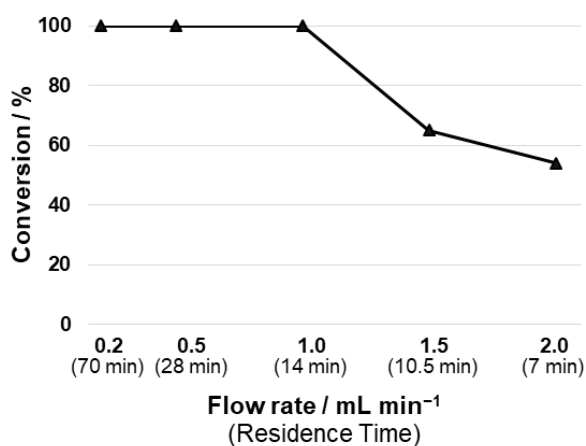


Figure 19. The effect of residence time on the homocoupling. Conditions: 1 equiv. 4-ethynyltoluene ($c=0.075$ M), 6 mol% CuBr₂, 0.5 equiv. TMEDA, 0.5 equiv. DIEA, DMSO as solvent, 120 °C

Investigation of the auxiliaries led to the conclusion that the amount of TMEDA and DIEA can be reduced to 0.25 equiv. without loss in conversion (Table 12, entries 1–2). It was also recognized that the joint application of the ligand and the base is crucial: the conversion decreased dramatically when using only TMEDA or DIEA as the sole additive (entries 4 and 5).

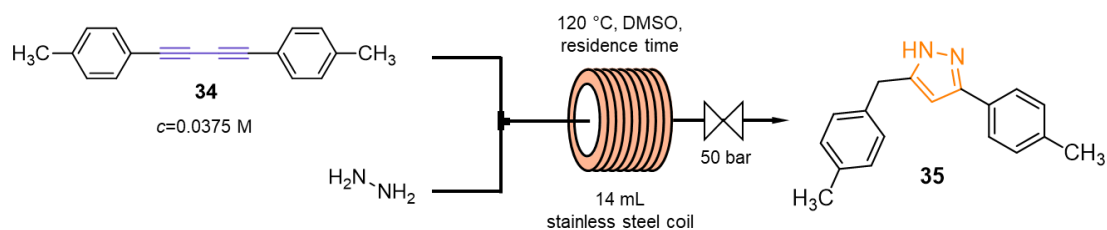
Table 12. The effect of auxiliaries on the homocoupling reaction of 4-ethynyltoluene. Conditions: 1 equiv. 4-ethynyltoluene ($c=0.075$ M), 6 mol% CuBr₂ as catalyst, DMSO as solvent, 120 °C, 1 mL min⁻¹ (14 min residence time)

Entry	TMEDA (equiv.)	DIEA (equiv.)	Conv. ^a (%)
1	0.5	0.5	100
2	0.25	0.25	100
3	0.1	0.1	30
4	0.25	0	20
5	0	0.25	16

^a Determined by ¹H NMR spectroscopy of the crude material. Chemoselectivity of diyne formation was 100% in all reactions.

The best conditions for the 1,3-dialkyne synthesis from 4-ethynyltoluene were as follows: 0.075 M alkyne concentration, 0.25 equiv. TMEDA, and 0.25 equiv. DIEA, DMSO as solvent, 120 °C, 1 mL min⁻¹ flow rate (14 min residence time).

Following the step-by-step optimization strategy, the Cope-type hydroamination was next studied utilizing preformed 1,4-di-*p*-tolylbuta-1,3-diyne as model compound. When the diyne and the hydrazine were combined and pumped together by means of a sole HPLC pump, uncontrollable gas formation occurred. Therefore, the stream of the diyne solution (0.0375 M in DMSO) was combined with the hydrazine stream (60 wt% aqueous solution containing 0.1125 M hydrazine in DMSO) in a T-mixer. The reaction mixture was pumped through a 14 mL reaction coil at 120 °C utilizing different flow rates (Scheme 12).



Scheme 12. Arrangement of the continuous-flow reactor for the hydroamination of 1,4-di-*p*-tolylbuta-1,3-diyne

It was found that the reaction is strongly dependent on the applied residence time. When both pumps were operated at 0.5 mL min⁻¹ (14 min residence time), a conversion of only 10% occurred (Figure 20). Decreasing the flow rate of both pumps to 0.1 mL min⁻¹ (70 min residence time) afforded 89% conversion resulting in the formation of the corresponding pyrazole as the only product. Bearing in mind the optimization of the individual reaction steps in the telescoped system, further lower flow rates were not investigated.

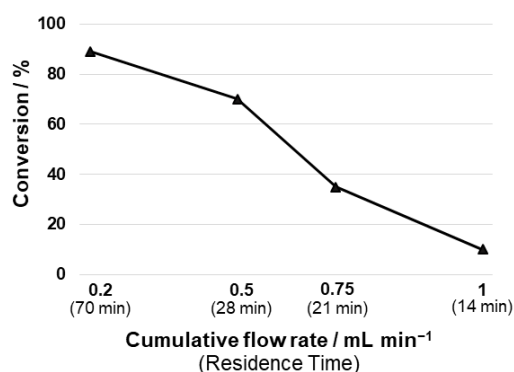
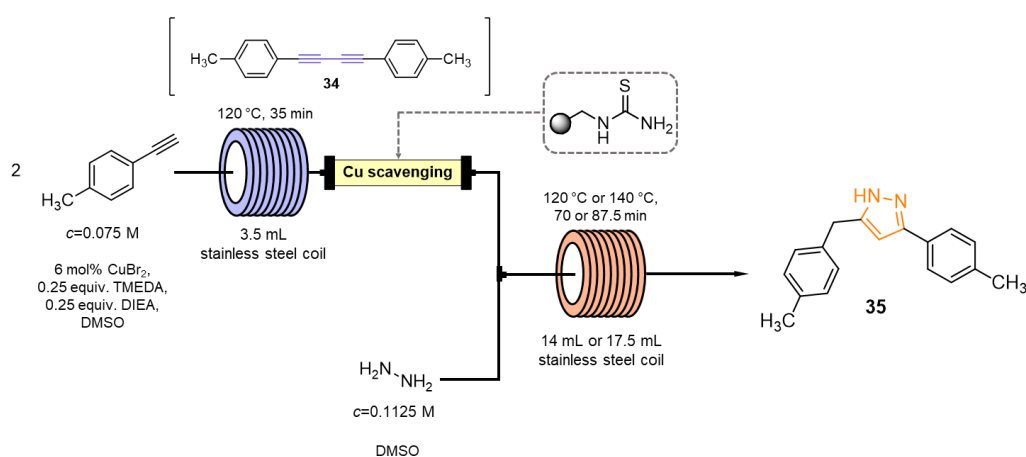


Figure 20. The effect of residence time in the model reaction of the hydroamination. Conditions: 1 equiv. diyne ($c = 0.0375$ M), 3 equiv. hydrazine ($c = 0.1125$ M), DMSO as solvent, 120 °C. Pumps were operated at the same flow rate (Chemoselectivity of pyrazole formation was 100% in all reactions)

4.3.2 Telescoped pyrazole synthesis

After the individual optimization of the copper-catalyzed alkyne homocoupling and the Cope-type hydroamination, the two reaction steps were performed in a consecutive manner (Scheme 13).

To be able to synchronize the residence times in the individual reactor components, a 0.075 M 4-ethynyltoluene solution was pumped through a 3.5 mL reaction coil with 0.1 mL min⁻¹ flow rate, which gave a residence time of 35 min. Right after the reactor zone where alkyne dimerization took place, a column was installed, packed with a thiourea-based scavenger resin to remove copper catalyst from the liquid phase. The resulting diyne stream was next combined with the hydrazine stream (60 wt% aqueous solution containing 0.1125 M hydrazine in DMSO) at a flow rate of 0.1 mL min⁻¹, and the reaction mixture entered a 14 mL heated coil at a cumulative flow of 0.2 mL min⁻¹ corresponding to a residence time of 70 min. Pyrazole formation took place in this second reactor.



Scheme 13. Sematic representation of the optimized in continuo 3,5-disubstituted pyrazole synthesis

When both coils were heated to 120 °C, the alkyne starting material transformed quantitatively and the corresponding pyrazole was formed in an amount of 76%, together with 24% of 1,4-di-*p*-tolylbuta-1,3-diyne (Table 13, entry 1). To increase the yield of the pyrazole product, the second reaction coil was exchanged to a 17.5 mL one allowing a residence time of 87.5 min (0.2 mL min⁻¹ cumulative flow rate). Thus, the amount of pyrazole increased to an extent of 86% at 120 °C (entry 2), and elevating the temperature in the extended coil from 120 °C to 140 °C led to a 98% pyrazole formation (entry 3; conversion of the starting alkyne was 100% in both cases).

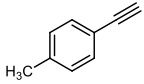
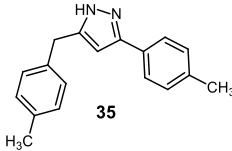
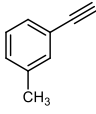
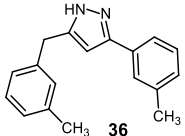
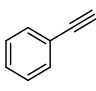
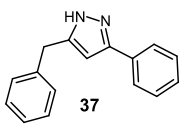

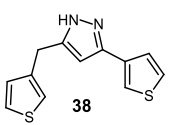
Table 13. Optimization of the hydroamination step of the consecutive model reaction. Conditions of the homocoupling: 1 equiv. 4-ethynyltoluene ($c=0.075\text{ M}$), 6 mol% CuBr_2 catalyst, DMSO as solvent, 120 °C, 35 min residence time. Conditions for hydroamination: 3 equiv. hydrazine ($c=0.1125\text{ M}$), DMSO as solvent

Entry	Temperature (°C)	Residence time (min)	Yield ^a (%)
1	120	70	76
2	120	87.5	86
3	140	87.5	98

^a NMR yield, determined by ¹H NMR spectroscopy of the crude material. No traces of unreacted alkyne were found in the crude material.

Subsequently, with the optimal conditions for the two-step pyrazole synthesis in hand, the scope and limits of the methodology were explored. Due to the fact that only homogeneous reaction mixtures can be applied in the CF system, certain alkynes with inappropriate solubility, such as 2- and 3-ethynylpyridine, could not be used as starting materials. Unfortunately, aliphatic alkynes such as 3-cyclohexyl-1-propyne and oct-1-yne resulted in unacceptable diyne formation and poor conversions to the pyrazole product, possibly because of the lack of conjugation. In these cases, further fine-tuning of the reaction conditions was necessary. However, applying phenylacetylene, its methyl-substituted derivatives, and 3-ethynylthiophene as starting alkynes, excellent results were registered (Table 14). The diyne formation took place quantitatively and no traces of unreacted alkyne were found in the crude material. As a result of the two-step synthesis, pyrazole products were achieved with full chemoselectivity, without side-product formation. After chromatographic purification, the corresponding pyrazoles were isolated in high yields (84–90%).

Table 14. Exploring the reactivity of different alkynes in the telescoped alkyne homocoupling–hydroamination/cyclization process. Conditions for the homocoupling: 1 equiv. alkyne ($c = 0.075\text{ M}$), 6 mol% CuBr_2 as catalyst, DMSO as solvent, $120\text{ }^\circ\text{C}$, 0.1 mL min^{-1} flow rate, 35 min residence time. Conditions for the hydroamination: 3 equiv. of hydrazine ($c = 0.1125\text{ M}$), DMSO as solvent, $140\text{ }^\circ\text{C}$, 0.1 mL min^{-1} flow rate, 87.5 min residence time

Entry	Starting material	Product	Yield ^a (%)
1			98 (90) ^b
2			90 (84) ^b
3			96 (84) ^b
4			94 (85) ^b

^a NMR yield, determined by ^1H NMR spectroscopy of the crude material. No traces of unreacted alkyne were found in the crude material. ^b Isolated yields indicated in parentheses.

Finally, the transformation of 3-ethynylthiophene was scaled out simply by elevating the operation time. Thus, the previously optimized conditions were applied without any change in the alkyne, ligand, base or hydrazine concentration. We were pleased to find that the flow system was stable for an extended period of 16 h. 0.52 g of pure 3-(thiophen-3-yl)-5-(thiophen-3-ylmethyl)-1*H*-pyrazole could be isolated, which corresponded to an overall yield of 81%.

5. SUMMARY

Recent dissertation collects knowledge and results earned during my PhD studies. We exploited the advantages of a strictly controlled flow reactor environment to explore novel parameter spaces and develop selective, inexpensive, and sustainable syntheses methods. Copper-catalyzed reactions were always in the center of our interest, thus, we investigated the CF technology in three copper-catalyzed reaction systems. Each study illustrated how CF processes can improve synthetic reaction technology.

Exploring the possibilities of the selective synthesis of aryl azides and aniline derivatives, a continuous-flow system was developed using the corresponding aryl halides as practical starting materials. Aryl azides and aryl amines were successfully prepared from the same starting materials using the same auxiliaries. Our results nicely demonstrated the synthetic usefulness of precise control over residence time and reaction temperature, thereby ensuring time-, cost-, and atom-efficient syntheses. It was established that after copper-mediated halogen–azide substitution, the azide decomposition/reduction is also dependent on the presence of the catalytic metal.

Subsequently, we utilized the reaction conditions of the model reaction for the synthesis of a diverse set of aromatic amines **2-15**. Gratifyingly, even *ortho*-substituted aryl bromides (**12**, **13**) were successfully transformed into the desired derivatives with 60–88% conversion and 100% selectivity. Selective synthesis of aryl azides proved to be more challenging, since it required an individual optimization of both the temperature and residence time for each substrate. However, we were pleased to find that after further optimization, azide **16-19** could also prepared with conversions of 83–96% and 82–100% selectivity.

With regard to the countless applications of aromatic azo compounds, we developed an efficient continuous-flow methodology for the selective and efficient synthesis of azobenzenes, employing copper powder as a cheap, readily available, nontoxic, and reusable catalytic source. Combining the application of overheated solvents and increased temperature and pressure ranges, our group revealed previously unknown correlations between reaction parameters that are not attainable in conventional flask chemistry and afforded a remarkable chemical intensification. Through this novel process window, we successfully extended the scope of the method to the synthesis of aromatic azo compounds **21-33**, with complete chemoselectivity and yields of 88–97%. Precise control of the residence time restricted the possibility of undesired reaction pathways, improving product selectivity and reducing waste generation.

As a consequence of a cooperation, we had the opportunity to investigate the inherently basic character of a copper-containing layered double hydroxide and successfully applied it as a catalytic source for the homocoupling of aniline derivatives without the need for any auxiliary substances. The resulting azobenzenes **20-30**, **32-33** were achieved with complete chemoselectivity and excellent, 91–98% yields in short process times even on preparative scales.

Utilizing our experiences in CF methodology and strategy, we constructed a two-step continuous-flow process for the synthesis of 3,5-disubstituted pyrazoles via sequential copper-mediated alkyne homocoupling and Cope-type hydroamination of the intermediary 1,3-dialkynes in the presence of hydrazine.

As a result of an initial step-by-step optimization procedure, we explored the optimum conditions of both the alkyne dimerization and the hydroamination. Next, the individual reaction components were organized into an uninterrupted flow sequence where, after in-line copper removal, the intermediary diynes were transformed further after being combined with a hydrazine stream. The developed process proved to be applicable for a range of aromatic alkynes and permitted a simple and easy access to a diverse set of pyrazoles **35-38** without the isolation of any intermediates. We were delighted to find that the reactions were chemoselective, no side-product formation was detected, isolated yields were in the range of 84–90%.

Acknowledgements

This work was carried out in the Institute of Pharmaceutical Chemistry, University of Szeged, during the years 2014–2018.

I would like to express my sincere gratitude to my supervisors *Prof. Dr. Ferenc Fülöp* and *Dr. Sándor Ötvös* for their professional guidance, useful advice, and constructive criticism. Their wisdom and honest thoughts helped me through many difficult decisions.

I am grateful to all former and current colleagues at the Institute of Pharmaceutical Chemistry, especially to *Rebeka Mészáros* and *Zsanett Szécsényi* for their help, friendship and, for providing me with a pleasant, unforgettable working atmosphere.

My special thanks goes to *Dr. Zsolt Szakonyi* for allowing the effective work in Laboratory No. 1.

I owe my thanks to *Prof. Árpád Molnár* for revising the English language of my thesis.

Finally, I would like to express my warmest thanks to my family and my friends, for their support during my PhD studies.

References

- [1] J. C. Warner, A. S. Cannon and K. M. Dye, *Environ. Impact Asses.* **2004**, *24*, 775-799.
- [2] R. Ciriminna and M. Pagliaro, *Org. Process Res. Dev.* **2013**, *17*, 1479-1484.
- [3] G. Jas and A. Kirschning, *Chem. Eur. J.* **2003**, *9*, 5708-5723.
- [4] V. Hessel, *Chem. Eng. Technol.* **2009**, *32*, 1655-1681.
- [5] J. Wegner, S. Ceylan and A. Kirschning, *Chem. Commun.* **2011**, *47*, 4583-4592.
- [6] C. Wiles and P. Watts, *Green Chem.* **2012**, *14*, 38-54.
- [7] P. H. Seeberger, *Nat. Chem.* **2009**, *1*, 258.
- [8] P. G. A., M. Debasis and O. M. G., *J. Flow Chem.* **2017**, *7*, 82-86.
- [9] D. E. Fitzpatrick, C. Battilocchio and S. V. Ley, *ACS Cent. Sci.* **2016**, *2*, 131-138.
- [10] J. Britton and C. L. Raston, *Chem. Soc. Rev.* **2017**, *46*, 1250-1271.
- [11] P. Bana, R. Örkényi, K. Lövei, Á. Lakó, G. I. Túrós, J. Éles, F. Faigl and I. Greiner, *Biorg. Med. Chem.* **2017**, *25*, 6180-6189.
- [12] S. A. Lawrence, *Amines : synthesis, properties, and applications*, Cambridge University Press, Cambridge, **2004**, p. x, 371 p.
- [13] S. Bräse, C. Gil, K. Knepper and V. Zimmermann, *Angew. Chem. Int. Ed.* **2005**, *44*, 5188-5240.
- [14] E. Merino and M. Ribagorda, *Beilstein J. Org. Chem.* **2012**, *8*, 1071-1090.
- [15] M. Roldo, E. Barbu, J. F. Brown, D. W. Laight, J. D. Smart and J. Tsibouklis, *Expert Opin. Drug Deliv.* **2007**, *4*, 547-560.
- [16] E. Merino, *Chem. Soc. Rev.* **2011**, *40*, 3835-3853.
- [17] K. Karrouchi, S. Radi, Y. Ramli, J. Taoufik, Y. Mabkhot, F. Al-aizari and M. Ansar, *Molecules* **2018**, *23*, 134.
- [18] S. Fustero, M. Sánchez-Roselló, P. Barrio and A. Simón-Fuentes, *Chem. Rev.* **2011**, *111*, 6984-7034.
- [19] L. Wang, X. Yu, X. Feng and M. Bao, *J. Org. Chem.* **2013**, *78*, 1693-1698.
- [20] A. S. Travis in *Manufacture and Uses of the Anilines: A Vast Array of Processes and Products, Vol.* **2009**.
- [21] Craig S. McKay and M. G. Finn, *Chem. Biol.* **2014**, *21*, 1075-1101.
- [22] W. Tang and M. L. Becker, *Chem. Soc. Rev.* **2014**, *43*, 7013-7039.
- [23] C. Yu, B. Liu and L. Hu, *J. Org. Chem.* **2001**, *66*, 919-924.
- [24] G. Wienhöfer, I. Sorribes, A. Boddien, F. Westerhaus, K. Junge, H. Junge, R. Llusar and M. Beller, *J. Am. Chem. Soc.* **2011**, *133*, 12875-12879.
- [25] T. Schabel, C. Belger and B. Plietker, *Org. Lett.* **2013**, *15*, 2858-2861.
- [26] H. Lu, Z. Geng, J. Li, D. Zou, Y. Wu and Y. Wu, *Org. Lett.* **2016**, *18*, 2774-2776.
- [27] C.-Z. Tao, X. Cui, J. Li, A.-X. Liu, L. Liu and Q.-X. Guo, *Tetrahedron Lett.* **2007**, *48*, 3525-3529.
- [28] H. Rao, H. Fu, Y. Jiang and Y. Zhao, *Angew. Chem. Int. Ed.* **2009**, *48*, 1114-1116.
- [29] K. D. Grimes, A. Gupte and C. C. Aldrich, *Synthesis* **2010**, *2010*, 1441-1448.
- [30] H.-L. Qi, D.-S. Chen, J.-S. Ye and J.-M. Huang, *J. Org. Chem.* **2013**, *78*, 7482-7487.
- [31] S. Voth, J. W. Hollett and J. A. McCubbin, *J. Org. Chem.* **2015**, *80*, 2545-2553.
- [32] N. Chatterjee, M. Arfeen, P. V. Bharatam and A. Goswami, *J. Org. Chem.* **2016**, *81*, 5120-5127.
- [33] G. D. Vo and J. F. Hartwig, *J. Am. Chem. Soc.* **2009**, *131*, 11049-11061.
- [34] D. Wang, Q. Cai and K. Ding, *Adv. Synth. Catal.* **2009**, *351*, 1722-1726.
- [35] H. Xu and C. Wolf, *Chem. Commun.* **2009**, 3035-3037.
- [36] Y. Aubin, C. Fischmeister, C. M. Thomas and J.-L. Renaud, *Chem. Soc. Rev.* **2010**, *39*, 4130-4145.

- [37] Z. Wu, Z. Jiang, D. Wu, H. Xiang and X. Zhou, *Eur. J. Org. Chem.* **2010**, 2010, 1854-1857.
- [38] X. Zeng, W. Huang, Y. Qiu and S. Jiang, *Org. Biomol. Chem.* **2011**, 9, 8224-8227.
- [39] C. Lombardi, J. Day, N. Chandrasoma, D. Mitchell, M. J. Rodriguez, J. L. Farmer and M. G. Organ, *Organometallics* **2017**, 36, 251-254.
- [40] W. Zhu and D. Ma, *Chem. Commun.* **2004**, 888-889.
- [41] J. Andersen, U. Madsen, F. Björkling and X. Liang, *Synlett* **2005**, 2005, 2209-2213.
- [42] Y. Goriya and C. V. Ramana, *Tetrahedron* **2010**, 66, 7642-7650.
- [43] J. T. Markiewicz, O. Wiest and P. Helquist, *J. Org. Chem.* **2010**, 75, 4887-4890.
- [44] S. Messaoudi, J.-D. Brion and M. Alami, *Adv. Synth. Catal.* **2010**, 352, 1677-1687.
- [45] Y. Chen, Z.-J. Zhuo, D.-M. Cui and C. Zhang, *J. Organomet. Chem.* **2014**, 749, 215-218.
- [46] A. R. Hajipour, M. Karimzadeh and S. Ghorbani, *Synlett* **2014**, 25, 2903-2907.
- [47] Z. Qin, I. Kastrati, R. E. P. Chandrasena, H. Liu, P. Yao, P. A. Petukhov, J. L. Bolton and G. R. J. Thatcher, *J. Med. Chem.* **2007**, 50, 2682-2692.
- [48] C. J. Drummond, F. Grieser and T. W. Healy, *J. Chem. Soc., Faraday Trans. 1* **1989**, 85, 561-578.
- [49] D. K. Hunger in *Dyes, General Survey, Vol.* Wiley-VCH Verlag GmbH & Co. KGaA, **2004**, pp. 1-12.
- [50] A. Simplicio, J. Clancy and J. Gilmer, *Molecules* **2008**, 13, 519-547.
- [51] A. Ryan, E. Kaplan, N. Laurieri, E. Lowe and E. Sim, *Sci. Rep.* **2011**, 1.
- [52] O. Wolk, S. Epstein, V. Ioffe-Dahan, S. Ben-Shabat and A. Dahan, *Expert Opin. Drug Deliv.* **2013**, 10, 1275-1286.
- [53] M. M. Patel, *Expert Opin. Drug Deliv.* **2014**, 11, 1343-1350.
- [54] S. K. Yesodha, C. K. Sadashiva Pillai and N. Tsutsumi, *Prog. Polym. Sci.* **2004**, 29, 45-74.
- [55] B. Sahraoui, J. Luc, A. Meghea, R. Czaplicki, J. L. Fillaut and A. Migalska-Zalas, *J. Opt. A: Pure Appl. Opt.* **2009**, 11, 024005.
- [56] Y. Takashima, S. Hatanaka, M. Otsubo, M. Nakahata, T. Kakuta, A. Hashidzume, H. Yamaguchi and A. Harada, *Nat Commun* **2012**, 3, 1270.
- [57] T. J. Kucharski, Y. Tian, S. Akbulatov and R. Boulatov, *Energy Environ. Sci.* **2011**, 4, 4449-4472.
- [58] Y. Feng, H. Liu, W. Luo, E. Liu, N. Zhao, K. Yoshino and W. Feng, *Sci. Rep.* **2013**, 3, 3260.
- [59] K. Masutani, M.-a. Morikawa and N. Kimizuka, *Chem. Commun.* **2014**, 50, 15803-15806.
- [60] B. Leipzig, *Z. Elektrochem.* **1898**, 4, 506-514.
- [61] B. Priewisch and K. Rück-Braun, *J. Org. Chem.* **2005**, 70, 2350-2352.
- [62] H.-U. Blaser, *Science* **2006**, 313, 312-313.
- [63] Y. Takeda, S. Okumura and S. Minakata, *Angew. Chem. Int. Ed.* **2012**, 51, 7804-7808.
- [64] S. Okumura, C.-H. Lin, Y. Takeda and S. Minakata, *J. Org. Chem.* **2013**, 78, 12090-12105.
- [65] K. Monir, M. Ghosh, S. Mishra, A. Majee and A. Hajra, *Eur. J. Org. Chem.* **2014**, 2014, 1096-1102.
- [66] L. Hu, X. Cao, L. Shi, F. Qi, Z. Guo, J. Lu and H. Gu, *Org. Lett.* **2011**, 13, 5640-5643.
- [67] L. Hu, X. Cao, L. Chen, J. Zheng, J. Lu, X. Sun and H. Gu, *Chem. Commun.* **2012**, 48, 3445-3447.
- [68] X. Liu, H.-Q. Li, S. Ye, Y.-M. Liu, H.-Y. He and Y. Cao, *Angew. Chem. Int. Ed.* **2014**, 53, 7624-7628.
- [69] A. Grirrane, A. Corma and H. García, *Science* **2008**, 322, 1661-1664.

- [70] S. Cai, H. Rong, X. Yu, X. Liu, D. Wang, W. He and Y. Li, *ACS Catal.* **2013**, *3*, 478-486.
- [71] W. Lu and C. Xi, *Tetrahedron Lett.* **2008**, *49*, 4011-4015.
- [72] C. Zhang and N. Jiao, *Angew. Chem. Int. Ed.* **2010**, *49*, 6174-6177.
- [73] Y. Zhu and Y. Shi, *Org. Lett.* **2013**, *15*, 1942-1945.
- [74] C. B. R. Reddy, S. R. Reddy and S. Naidu, *Catal. Commun.* **2014**, *56*, 50-54.
- [75] J. Wang, J. He, C. Zhi, B. Luo, X. Li, Y. Pan, X. Cao and H. Gu, *RSC Advances* **2014**, *4*, 16607-16611.
- [76] M. Naim, O. Alam, F. Nawaz, M. Alam and P. Alam, *J. Pharm. Bioallied Sci.* **2016**, *8*, 2-17.
- [77] O. I. El-Sabbagh, M. M. Baraka, S. M. Ibrahim, C. Pannecouque, G. Andrei, R. Snoeck, J. Balzarini and A. A. Rashad, *Eur. J. Med. Chem.* **2009**, *44*, 3746-3753.
- [78] D. Havrylyuk, B. Zimenkovsky, O. Vasylenko, A. Gzella and R. Lesyk, *J. Med. Chem.* **2012**, *55*, 8630-8641.
- [79] H. Kumar, D. Saini, S. Jain and N. Jain, *Eur. J. Med. Chem.* **2013**, *70*, 248-258.
- [80] V. Kumar, K. Kaur, G. K. Gupta and A. K. Sharma, *Eur. J. Med. Chem.* **2013**, *69*, 735-753.
- [81] H. K. Maurya, R. Verma, S. Alam, S. Pandey, V. Pathak, S. Sharma, K. K. Srivastava, A. S. Negi and A. Gupta, *Bioorg. Med. Chem. Lett.* **2013**, *23*, 5844-5849.
- [82] A. Schmidt and A. Dreger, *Curr. Org. Chem.* **2011**, *15*, 1423-1463.
- [83] E. Gondek, *Mater. Lett.* **2013**, *112*, 94-96.
- [84] L. Knorr, *Ber. Dtsch. Chem. Ges.* **1883**, *16*, 2597-2599.
- [85] B. A. Bhat, S. C. Puri, M. A. Qurishi, K. L. Dhar and G. N. Qazi, *Synth. Commun.* **2005**, *35*, 1135-1142.
- [86] F. Gosselin, P. D. O'Shea, R. A. Webster, R. A. Reamer, R. D. Tillyer and E. J. J. Grabowski, *Synlett* **2006**, *2006*, 3267-3270.
- [87] L. M. Oh, *Tetrahedron Lett.* **2006**, *47*, 7943-7946.
- [88] X. Qi and J. M. Ready, *Angew. Chem. Int. Ed.* **2007**, *46*, 3242-3244.
- [89] T. Delaunay, P. Genix, M. Es-Sayed, J.-P. Vors, N. Monteiro and G. Balme, *Org. Lett.* **2010**, *12*, 3328-3331.
- [90] V. K. Rao, R. Tiwari, B. S. Chhikara, A. N. Shirazi, K. Parang and A. Kumar, *RSC Advances* **2013**, *3*, 15396-15403.
- [91] Y. Wang, D. Wei, W. Zhang, Y. Wang, Y. Zhu, Y. Jia and M. Tang, *Org. Biomol. Chem.* **2014**, *12*, 7503-7514.
- [92] J. Comas-Barcelo, D. Blanco-Ania, S. A. M. W. van den Broek, P. J. Nieuwland, J. P. A. Harrity and F. P. J. T. Rutjes, *Catal. Sci. Technol.* **2016**, *6*, 4718-4723.
- [93] A. DeAngelis, D.-H. Wang and S. L. Buchwald, *Angew. Chem. Int. Ed.* **2013**, *52*, 3434-3437.
- [94] I. R. Baxendale, S. C. Schou, J. Sedelmeier and S. V. Ley, *Chem. Eur. J.* **2010**, *16*, 89-94.
- [95] J.-S. Poh, D. L. Browne and S. V. Ley, *React. Chem. Eng.* **2016**, *1*, 101-105.
- [96] B. Li, D. Widlicka, S. Boucher, C. Hayward, J. Lucas, J. C. Murray, B. T. O'Neil, D. Pfisterer, L. Samp, J. VanAlsten, Y. Xiang and J. Young, *Org. Process Res. Dev.* **2012**, *16*, 2031-2035.
- [97] K. P. Cole, J. M. Groh, M. D. Johnson, C. L. Burcham, B. M. Campbell, W. D. Diserod, M. R. Heller, J. R. Howell, N. J. Kallman, T. M. Koenig, S. A. May, R. D. Miller, D. Mitchell, D. P. Myers, S. S. Myers, J. L. Phillips, C. S. Polster, T. D. White, J. Cashman, D. Hurley, R. Moylan, P. Sheehan, R. D. Spencer, K. Desmond, P. Desmond and O. Gowran, *Science* **2017**, *356*, 1144-1150.
- [98] M. B. Plutschack, B. Pieber, K. Gilmore and P. H. Seeberger, *Chem. Rev.* **2017**.

- [99] T. Razzaq and C. O. Kappe, *Chem. Asian J.* **2010**, *5*, 1274-1289.
- [100] S. V. Ley, D. E. Fitzpatrick, R. J. Ingham and R. M. Myers, *Angew. Chem. Int. Ed.* **2015**, *54*, 3449-3464.
- [101] I. R. Baxendale, *J. Chem. Technol. Biotechnol.* **2013**, *88*, 519-552.
- [102] F. Darvas, V. Hessel and G. Dorman, *Flow Chemistry Volume 1 - Fundamentals*, De Gruyter, **2014**, p.
- [103] I. M. Mándity, S. B. Ötvös and F. Fülöp, *ChemistryOpen* **2015**, *4*, 212-223.
- [104] J.-I. Yoshida, *Chem. Rec.* **2010**, *10*, 332-341.
- [105] A. Nagaki, S. Yamada, M. Doi, Y. Tomida, N. Takabayashi and J.-i. Yoshida, *Green Chem.* **2011**, *13*, 1110-1113.
- [106] T. Schwalbe, V. Autze and G. Wille, *CHIMIA* **2002**, *56*, 636-646.
- [107] A. J. DeMello, *Nature* **2006**, *442*, 394-402.
- [108] V. Hessel, D. Kralisch, N. Kockmann, T. Noël and Q. Wang, *ChemSusChem* **2013**, *6*, 746-789.
- [109] G. M. Keser, T. Soos and C. O. Kappe, *Chem. Soc. Rev.* **2014**, *43*, 5387-5399.
- [110] P. D. Morse, R. L. Beingessner and T. F. Jamison, *Isr. J. Chem.* **2017**, *57*, 218-227.
- [111] V. H. Timothy Noel in *Chemical Intensification in Flow Chemistry through Harsh Reaction Conditions and New Reaction Design*, Vol. (Ed. W. Reschetilowski), Wiley-VCH, Weinheim, **2013**, pp. 273-295.
- [112] A. Adeyemi, J. Bergman, J. Brånalt, J. Sävmarker and M. Larhed, *Org. Process Res. Dev.* **2017**, *21*, 947-955.
- [113] R. Porta, M. Benaglia and A. Puglisi, *Org. Process Res. Dev.* **2016**, *20*, 2-25.
- [114] J. Wegner, S. Ceylan and A. Kirschning, *Adv. Synth. Catal.* **2012**, *354*, 17-57.
- [115] B. Pieber, K. Gilmore and P. H. Seeberger, *J. Flow Chem.* **2017**, 1-8.
- [116] P. Zhang, M. G. Russell and T. F. Jamison, *Org. Process Res. Dev.* **2014**, *18*, 1567-1570.
- [117] T. Tsubogo, H. Oyamada and S. Kobayashi, *Nature* **2015**, *520*, 329-332.
- [118] A. Adamo, R. L. Beingessner, M. Behnam, J. Chen, T. F. Jamison, K. F. Jensen, J.-C. M. Monbaliu, A. S. Myerson, E. M. Revalor, D. R. Snead, T. Stelzer, N. Weeranoppanant, S. Y. Wong and P. Zhang, *Science* **2016**, *352*, 61-67.
- [119] H. Zhao, H. Fu and R. Qiao, *J. Org. Chem.* **2010**, *75*, 3311-3316.
- [120] G. L'Abbe, *Chem. Rev.* **1969**, *69*, 345-363.
- [121] G. L'Abbe and G. Mathys, *J. Org. Chem.* **1974**, *39*, 1778-1780.
- [122] H. Kwart and A. A. Kahn, *J. Am. Chem. Soc.* **1967**, *89*, 1950-1951.
- [123] H. Peng, K. H. Dornevil, A. B. Draganov, W. Chen, C. Dai, W. H. Nelson, A. Liu and B. Wang, *Tetrahedron* **2013**, *69*, 5079-5085.
- [124] K. Alfonsi, J. Colberg, P. J. Dunn, T. Fevig, S. Jennings, T. A. Johnson, H. P. Kleine, C. Knight, M. A. Nagy, D. A. Perry and M. Stefaniak, *Green Chem.* **2008**, *10*, 31-36.
- [125] S. B. Ötvös, I. Pálkó and F. Fülöp, *Catal. Sci. Technol.* **2019**, *9*, 47-60.
- [126] S. B. Ötvös, Á. Georgiádes, M. Ádok-Sipiczki, R. Mészáros, I. Pálkó, P. Sipos and F. Fülöp, *Appl. Catal. A Gen.* **2015**, *501*, 63-73.

Appendix